1983

Design parameters for filter capacity

Myong Jin Yu
Iowa State University

Yu, Myong Jin

DESIGN PARAMETERS FOR FILTER CAPACITY

Iowa State University PH.D. 1983

PLEASE NOTE:

In all cases this material has been filmed in the best possible way from the available copy. Problems encountered with this document have been identified here with a check mark __✓__.

1. Glossy photographs or pages _____
2. Colored illustrations, paper or print _____
3. Photographs with dark background _____
4. Illustrations are poor copy _____
5. Pages with black marks, not original copy _____
6. Print shows through as there is text on both sides of page _____
7. Indistinct, broken or small print on several pages ✓
8. Print exceeds margin requirements _____
9. Tightly bound copy with print lost in spine _____
10. Computer printout pages with indistinct print _____
11. Page(s) _____ lacking when material received, and not available from school or author.
12. Page(s) _____ seem to be missing in numbering only as text follows.
13. Two pages numbered _____. Text follows.
14. Curling and wrinkled pages _____
15. Other _____

Design parameters for filter capacity

by

Myong Jin Yu

A Dissertation Submitted to the

Graduate Faculty in Partial Fulfillment of the

Requirements for the Degree of

DOCTOR OF PHILOSOPHY

Department: Civil Engineering
Major: Sanitary Engineering

Approved:

Signature was redacted for privacy.

In Charge of Major Work

Signature was redacted for privacy.

For the Major Department

Signature was redacted for privacy.

For the Graduate College

Iowa State University
Ames, Iowa

1983

TABLE OF CONTENTS

LIST OF FIGURES

LIST OF TABLES

INTRODUCTION

Many mathematical models have been proposed to describe the deep bed filtration process since Iwasaki (26) first introduced his mathematical expressions for the kinetics and conservation of mass in sand filtration. In general, solutions of mathematical models relate the effluent suspended solids concentration to input variables including service time, filter depth, filtration rate and influent suspended solids concentration. Therefore, they should provide a useful tool for interpreting the effects of design variables on the filtration process and for predicting the performance of a filter design.

Saatci and Oulman (42, 43, 44) developed a Bed Depth Service Time (BDST) type method based on the similarities between adsorption and filtration. Their model provides design parameters for estimating the solids retention characteristics of a deep bed filter by a simple curve fitting of data obtained from a pilot plant filter. The design parameters obtained from this curve fitting method were expected to be useful in the design of deep bed filters. However, it is apparent that the design parameters in the BDST method are not constants but should be affected by both the suspended solids concentration and filtration rate.

In this study, a kinetic equation applicable to the filtration process will be considered in a semi-empirical manner. Many physical and chemical factors affect filtration performance by changing the solids retention characteristics of the filter. Therefore, the effects of some of the variables such as filtration rate, media size and influent suspended solids concentration on the filter performance will be studied while maintaining other variables constant.

Pilot plants are widely used to guide the design and operation of filters. There would be savings in time and work involved if shallow depth filters can be used instead of full depth filters in the pilot plant. The effects of filter depth will be investigated to determine whether the depth of the filter affects the design parameters.

Specifically, the objectives of this study were:

a) to evaluate the suitability of the kinetic equation expressed by the limited growth concept,

b) to evaluate the factors affecting filter performance by estimating the effects of parameters such as filtration rate, influent suspended solids concentration, media grain size, and filter depth on the attachment coefficient and filter capacity,

c) to develop a head loss equation related to the filtration coefficients.

To accomplish these objectives, a pilot plant was

operated consisting of a mixing tank and five filter columns with piezometers to measure the head losses through the filters. Three different sand sizes were used as filter media with mean diameter ranging from 0.59 mm to 1.19 mm. Runs were made with iron concentrations ranging from 4 to 8 mg/l. In each run, parallel operations with three different filtation rates and one media size and with three different media sizes and the same filtration rate were conducted to obtain comparable data for a given suspension of iron. The filtration coefficients for various depths of pilot filters were evaluated to determine whether the performance of full depth filters could be predicted from tests made using thin layer filters. A sensitivity analysis of attachment coefficient and filter capacity was used to evaluate the effects of these parameters on filter performance. It was found that the filter capacity was highly dependent on the influent suspended solids concentration, filtration rate and filter depth but the attachment coefficient was not. It was also apparent that both head loss and effluent quality are strongly affected by media size but that the breakthrough curve equations do not adequately predict the effects of media size at the present time.

LITERATURE REVIEW

Mass Balance and Kinetic Equations of Filtration

The hypothesis used by many researchers to explain filtration is that the removal of a suspension with respect to depth in the filter is a first order process:

$$-\frac{\partial C}{\partial x} = \lambda C \qquad (1)$$

where

C = suspended solids concentration

x = distance in the direction of flow

λ = a filter coefficient.

Another basic equation that is widely used is the mass balance equation for the solids being removed:

$$-V\frac{\partial C}{\partial x} = \frac{\partial \sigma}{\partial t} \qquad (2)$$

where

V = filtration rate

σ = specific deposit

t = time.

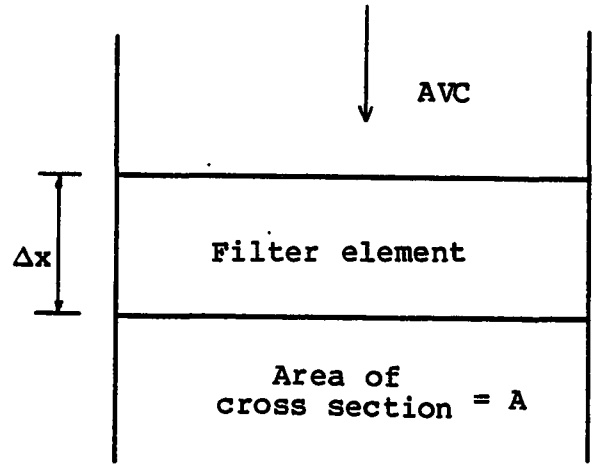

Figure 1. Filter element

These two equations were first used to model the filtration process by Iwasaki (26). Since then, kinetic equations analogous to Equation 1 have been used (50, 12, 18, 19, 24, 31, 32, 14).

Herzig et al. (15) defined the retention probability, q, of particles in an element of a filter bed (Figure 1) with an area, A, and depth, Δx, as:

$$q = \frac{A\ \Delta x\ \frac{\partial \sigma}{\partial t}\ \Delta t}{AVC\ \Delta t}$$

$$= \frac{\Delta x}{VC} \frac{\partial \sigma}{\partial t}$$

Thus, the retention probability per unit of depth, k, would be:

$$k = \frac{1}{VC} \frac{\partial \sigma}{\partial t} \qquad (3)$$

Equation 3 can be rewritten as:

$$\frac{\partial \sigma}{\partial t} = kVC \qquad (4)$$

Equation 4 is analogous to the classical equation of chemical kinetics and for this reason it is called the kinetic equation.

The general mass balance equation is:

accumulation rate = input rate - output rate

In terms of the filtration variables, the mass balance equation is:

$$\frac{\partial}{\partial t} A(\sigma + C) + \frac{\partial}{\partial x} (AVC - AD \frac{\partial C}{\partial x}) = 0$$

where

ϵ = porosity

D = diffusion coefficient.

For a constant filtration rate, the exact form of the mass balance equation for the particles is:

$$\frac{\partial}{\partial t}(\sigma + C) + V\frac{\partial C}{\partial x} - D\frac{\partial^2 C}{\partial x^2} = 0$$

Particle diffusion is virtually negligible when the particle size is larger than 1 micron. For particles in this size range, the mass balance equation becomes:

$$\frac{\partial}{\partial t}(\sigma + C) + V\frac{\partial C}{\partial x} = 0 \qquad (5)$$

Combining Equation 1 and Equation 5:

$$\frac{\partial}{\partial t}(\sigma + C) = \lambda V C$$

which is a kinetic expression for the whole quantity of particles (moving and retained) and the suspension concentration. Herzig et al. claimed that Equation 1 could not be a kinetic equation, since only retained particles can be taken into account for clogging. However, it is often

assumed that the moving particles may be neglected because of the overwhelming effects of the retained particles. Then, the mass balance equation reduces to Equation 2 which has been used for most of the filtration models. Combining Equation 1 and Equation 2:

$$\frac{\partial \sigma}{\partial t} = \lambda V C \tag{6}$$

This is the equivalent to Equation 4 where λ is identical to k.

Not all authors of mathematical models have used either Equation 1 or Equation 4. Mints (33) insisted that spontaneous detachment occurs during filtration and that deposits accumulated in the depth of a filter medium have a structure that is not uniformly strong. Under the action of hydrodynamic forces due to the velocity of water through the medium, which increases in proportion to the head losses, this structure may be partly destroyed. Part of the particles that are less strongly attached to the filter grains may become detached. The equation proposed by Mints and Krishtul (34) to account for this detachment has the form:

$$- \frac{\partial C}{\partial x} = bC - \frac{a}{\nabla} \sigma \tag{7}$$

where a and b are constants. According to Equation 7, continuous detachment should be observed even during the passage of clean water through a clogged filter. However, Mackrle did not observe any measurable detachment when he passed clean water without interrupting or changing the flow rate through a highly clogged filter. Mints responded that deposition is dynamic and that detachment can only take place with on-going deposition (33,57).

Mints et al. (35) performed filtration runs to show the phenomenon of particle detachment. Their filter had a depth of 3.3 cm of 1.5 mm sand in a 24 cm long glass tube with a diameter of 3.3 cm. Water containing 100 units of color was filtered through the sand at a filtration rate of 8.25 m/hr. A coagulant dose of 12.5 mg/1 of alum (as Al_2O_3) was added at the entrance to the column. For the first 15 minutes, no flocs were observed in the filtrate, but later small flocs started to appear. Gradually, as sediment accumulated in the layer and as head loss increased, the rate of floc detachment also increased. Then, filtration of colored water with coagulant was stopped, and the filtration of clear water was begun. At the same flow rate as before, the detachment of flocs ceased. Mints concluded that the detachment of flocs could take place only during continuous formation of sediment and/or when the head loss is increasing.

Stanley (49) operated a filter for 151 minutes, using

hydrous ferric oxide floc labelled with radioactive I^{131}. When he changed the suspension to one which had no radioactive label, but which was otherwise identical, he found that none of the floc deposited in the early part of filter run was detached and redeposited or carried out with the filtrate. This evidence in a dynamic filtration situation that detachment did not take place contradicts Mints' deposition and scour hypothesis. Mints attributed particles in the filtrate that were visually larger than those entering the layer to being scoured particles from the deposits. It is also possible, however, that they might be formed by flocculation as Ives has claimed (57).

If attachment and detachment are simultaneous as in Mints' hypothesis, the kinetic equation could also be written in a form that has been published by Herzig et al. (15).

$$\frac{\partial \sigma}{\partial t} = kVC - k_d\sigma \qquad (8)$$

where k_d is a detachment coefficient.
Since a kinetic equation based on attachment-detachment hypothesis is difficult to integrate, and since proof of spontaneous detachment has yet to be demonstrated, it probably is not worthwhile to include the detachment term.

Most proponents of filtration models have assumed that the filter coefficient, λ, is not constant but is some

function of specific deposit, σ. They have assumed, however, that λ is independent of suspended solids concentration, C. Iwasaki (26) assumed that λ might gradually increase during filtration as the void spaces in the sand layer become filled with deposits.

Ives (18) considered the filter coefficient, λ, to be a function of interstitial velocity, grain surface area and Stokes law parameters of the water and suspended particles. Initially, the deposits form dome shaped caps on the filter grain surfaces and this increases the surface area available for deposition. Thus, λ increases linearly with the deposition of solids in the filter:

$$\lambda = \lambda_o + r\sigma \tag{9}$$

where

r = constant

λ_o = initial filter coefficient.

Increasing deposition causes the pores to become gradually constricted, tending to

a) straighten the flow streamlines,

b) increase the interstitial velocity,

c) reduce the interstitial surface area.

Each of these actions reduces the deposition rate so that λ

diminishes. Equation 9 may be modified to:

$$\lambda = \lambda_o + r\sigma - \frac{s\sigma^2}{\epsilon_o - \sigma} \tag{10}$$

where s is a constant.

Maroudas and Eisenklam (32) developed models based on the hypothesis that no further deposition would take place when the interstitial velocity reached a critical velocity. Thus, λ_o and λ are functions of these velocity terms:

$$\lambda_o = k(\frac{1}{u_o} - \frac{1}{u_c}) \tag{11}$$

and

$$\lambda = k(\frac{1}{u} - \frac{1}{u_c}) \tag{12}$$

where

k = constant

u = interstitial velocity

u_o = initial interstitial velocity

u_c = critical interstitial velocity.

Then,

$$\lambda = \lambda_o(u_c/u - 1)/(u_c/u_o - 1) \tag{13}$$

They assumed that the fractional volume of blocked flow paths, n, progressively increases during filtration until n reaches n^* which is the value of n at the nonretaining state.

Then

$$\frac{u}{u_o} = \frac{V/\epsilon}{V/\epsilon_o}$$

$$= \frac{\epsilon_o}{\epsilon}$$

$$= \frac{1}{1 - n} \qquad (14)$$

and

$$\frac{u_c}{u_o} = \frac{1}{1 - n^*} \qquad (15)$$

Substituting Equations 14 and 15 into Equation 13:

$$\frac{\lambda}{\lambda_o} = 1 - \frac{n}{n^*}$$

Then, the kinetic equation becomes

$$\frac{\partial C}{\partial x} = -\lambda_o (1 - \frac{n}{n^*}) \qquad (16)$$

They formulated a deposition equation such that:

$$\frac{1}{1 - n} \frac{\partial \sigma}{\partial t} = \beta \frac{\partial n}{\partial t} \tag{17}$$

where

β = a deposition coefficient (the volume of particles required to block a unit volume of bed).

By solving Equations 16 and 17 with the mass balance equation, Equation 2, they were able to determine n and C in terms of x and t.

In Heertjes and Lerk's hypothesis (14), a deep bed filter is considered to be composed of unit-cells that are followed by a mixing-cell. In each unit cell, laminar flow dominates. Particles are attracted by London-van der Waals forces and are removed by adhesion to filter grain surface. Their final kinetic equation was:

$$- \frac{\partial C}{\partial x} = K(\epsilon_o - \sigma)C \tag{18}$$

By solving this kinetic equation and the mass balance equation, Equation 2, they obtained:

$$C = \frac{C_o}{1 + \exp\ (-VC_oKt)\left[\exp\ (K\epsilon_o x) - 1\right]} \tag{19}$$

$$\sigma = \frac{\epsilon_o}{1 + \frac{\exp\ (K\epsilon_o x)}{\exp\ (VC_o Kt) - 1}} \tag{20}$$

where C_o is influent suspended solids concentration.

If we combine Equation 18 with Equation 2:

$$\frac{\partial \sigma}{\partial t} = KV(\epsilon_o - \sigma)C \tag{21}$$

We find that Equation 21 is identical with the equation for the limited growth model if ϵ_o is ultimate capacity.

If $\exp\ (K\epsilon_o x) << 1$, Equation 19 becomes (14):

$$\ln\ (\frac{C_o}{C} - 1) = K\epsilon_o x - VC_o Kt$$

or

$$x = \frac{VC_o}{\epsilon_o} t + \frac{1}{K\epsilon_o} \ln\ (\frac{C_o}{C} - 1) \tag{22}$$

C was expressed as the volume of solids per unit volume of suspension in the preceding equations. Introducing the concentration measured in weight per unit volume, $(C)_g$,

$$C = w(C)_g$$

where w is the reciprocal of the density of the suspended solids. Then, Equation 22 becomes:

$$x = \frac{Vw}{\epsilon_o} (C_o)_g t + \frac{1}{K\epsilon_o} \ln \left[\frac{(C_o)_g}{(C)_g} - 1\right]$$

They plotted $(C_o)_g t$ versus x, from this plot determined the density of the suspended solids, (1/w), and the filtration constant, K.

Ives (20) formulated the most general of all the variously proposed equations to predict the filter coefficient.

$$\lambda = \lambda_o(1 - \sigma/\sigma_u)^x(1 + \beta\sigma/\epsilon_o)^y(1 - \sigma/\epsilon_o)^z \qquad (23)$$

where β, x, y and z are constants.

Equation 23 is not based on a detailed examination of the filtration mechanisms, but on more general assumptions of the importance of pore geometry and interstitial velocity. Initially, deposits on the grains will cause the spherical model to dominate but, as deposits become contiguous, side spaces will be filled with solids and flow will be through channels approximating capillaries. The first term of Equation 23 was based on the Maroudas model and the last two terms were based on the sphere and capillary model proposed by Mackrle. Assuming that λ is proportional to some power

of the difference between the reciprocals of the interstitial and critical velocities:

$$\lambda \propto \left[\frac{1}{u} - \frac{1}{u_c}\right]^x$$

or

$$\lambda \propto \left[\frac{\epsilon_o - \sigma}{V} - \frac{\epsilon_o - \sigma_u}{V}\right]^x$$

or

$$\lambda \propto \left[\frac{\sigma_u - \sigma}{V}\right]^x$$

Consequently,

$$\frac{\lambda}{\lambda_o} \propto \left[\frac{\sigma_u - \sigma}{\sigma_u}\right]^x$$

or

$$\frac{\lambda}{\lambda_o} \propto (1 - \sigma/\sigma_u)^x$$

Most of previous models of the filtration coefficient can be expressed by the Ives equation by making a suitable choice of the exponents x, y, z. Heertjes and Lerk's model can be represented by Ives's general equation where $x = y = 0$ and

z = 1, resulting in:

$$\frac{\lambda}{\lambda_o} = (1 - \sigma/\epsilon_o)$$

An advantage of the Heertjes and Lerk model is that explicit solutions such as Equations 19 and 20 can be obtained easily, and the filtration constant can be found by simple regression.

Some others (2,42) have used kinetic equations similar to those developed for adsorption and ion exchange. They thought they could explain deep bed filtration by modifying the models for adsorption and ion exchange to accommodate the differences between these processes.

Adin and Rebhun (2) proposed the following kinetic equation:

$$\frac{\partial\sigma}{\partial t} = k_1 VC(F - \sigma) - k_2\sigma J \qquad (24)$$

where

k_1 = an attachment coefficient

k_2 = a detachment coefficient

F = the theoretical filter capacity

J = the hydraulic gradient.

This equation is similar to the equation which Thomas (54)

used to describe the kinetics of adsorption:

$$\frac{\partial q}{\partial t} = k_1(a - q)C - k_2 q \qquad (25)$$

where

k_1, k_2 = velocity constants

a = total adsorption capacity

q = concentration of adsorbed material.

In an adsorption bed, the porosity remains constant throughout the whole run, but in filtration, particles accumulate in the filter pores and consequently the head loss increases. Adin and Rebhun thought that detachment would not be simply proportional to the specific deposit so they introduced the hydraulic gradient into the detachment term. Adin (1) solved Equation 24 and his material balance equation on a computer using numerical analysis methods.

Saatci (42) pointed out that the effect of the hydraulic gradient in Equation 24 is not significant in the early stages of filtration. He used Equation 25 which does not have a hydraulic gradient term and developed an analytical solution by combining the simplified kinetic equation with a material balance equation. He then assumed that detachment is negligible (i.e., $k_2 <<< k_1$) and obtained:

$$\frac{C}{C_o} = \frac{1}{1 + \exp\ (k_1 \epsilon_o x/V - k_1 C_o t)} \qquad (26)$$

Then, he replaced the initial porosity, ϵ_o, by the initial filter capacity, F_o, a variable which seems to be different from ϵ_o. He rearranged Equation 26 as follows:

$$t = \frac{F_o}{C_o V}\left[x - \frac{V}{K_1 F_o} \ln \left[\frac{C_o}{C} - 1\right]\right] \qquad (27)$$

The Bohart Adams equation (5), published in 1920 was used as the basis for the more recent BDST method (16). The Bohart Adams equation is:

$$\frac{C}{C_o} = \frac{\exp\ (KC_o t)}{\exp\ (Ka_o x/V) - 1 + \exp\ (KC_o t)}$$

where a_o is initial volume chlorine capacity of charcoal. Since $\exp\ (Ka_o x/v) >>> 1$, their results can be written as

$$t = \frac{a_o}{C_o V}\left[x - \frac{V}{Ka_o} \ln\ (\frac{C_o}{C} - 1)\right]$$

Therefore, Equation 27 is identical to the Bohart Adams Equation if $F_o = a_o$. Saatci applied the BDST method to analyze his filtration data.

Saleh (46) proposed a kinetic equation which is quite different in form:

$$\frac{\partial \sigma}{\partial t} = \frac{KV}{J}(\sigma_u - \sigma)C \qquad (28)$$

Adin and Rebhun, Saatci, and Saleh all used the volumetric filter capacity available for particle deposition, $F - \sigma$, $F_o - \sigma$ or $\sigma_u - \sigma$, as the basis of a limited growth model, which is appropriate to describe a monolayer adsorption process. But, filtration is more similar to multilayer adsorption. Therefore, the surface area should be considered to be a measure of the available sites for deposition instead of a measure of the volumetric capacity that is remaining. The kinetic equations developed by Adin and Rebhun, Saatci, and Saleh all are similar in form to those in the Heertjes model and in the Maroudas model as it was modified by Ives. However, each of these models is based on completely different hypotheses. Saleh's hypothesis was that the rate of particle deposition is proportional to the space available for particle deposition, $\sigma_u - \sigma$, and is inversely proportional to the hydraulic gradient. Saleh did not include a detachment term. Saatci's hypothesis was that the rate of particle deposition is proportional to $F_o - \sigma$, and that the rate of detachment is proportional to the amount of deposits. But Saatci assumed that the detachment to be negligible in his final analysis of data. Adin and Rebhun's hypothesis was that the rate of deposition is proportional to $F - \sigma$, and that the rate of detachment is proportional to

both the amount of deposits and the hydraulic gradient. It should be noted that σ_u, F_o, F all represent limiting values for the porosity for a clogged filter.

Initially, a filter which has been used for several filtration and backwash cycles has effluent of relatively poor quality. The improvement in quality that initially occurs in the filter run is frequently referred to as "filter ripening". The initial poor quality of the effluent during the ripening period is supposedly caused by remnants of the backwash water in the filter system or by unfavorable surface conditions of the partially cleaned filter grains. Amirtharajah and Wetstein (3) have illustrated how the filtration rate, influent suspended solids concentration and the rate of backwash valve closure can all affect the effluent quality during the ripening period and the length of that period.

Ives (18) and Tien et al. (56) attempted to describe the ripening period by relating the filtration coefficient to the active surface area for deposits. According to Ives, there is an increase in the specific surface due to the buildup of deposited particles on the filter medium grains and therefore, the filtration efficiency improves in the early stage of filtration. Tien et al. assumed that there are two stages of deposit morphologies: formation of a smooth coating during the early clean bed stage and blocking of

pores during the clogged bed stage. The active filter surface increases during the smooth coating stage but decreases during the clogged bed stage. Therefore, they proposed that λ increases in the early stages of filtration and then decreases during the later stages. Most of the other filtration models cannot describe the initial ripening period, but emphasize only the degradation of effluent quality which follows the ripening period. But, it is still not known whether the ripening period is caused by insufficient backwashing or by improvements in removal attributable to the increase in specific surface or by changes of surface properties of the collector surface.

Parameters Affecting the Filtration Coefficient

There are a number of physical and chemical factors that can affect the filtration coefficient, λ. The physical factors include filtration rate, media grain size, influent suspended solids concentration, suspended solids particle size and temperature. The chemical factors include pH, ionic strength and ionic species in the suspension, and types and dose of filter aids. Jackson (27, 28) has written extensively about the effects of these factors on filter performance in his reviews on granular media filtration.

It is generally accepted that the capture of fine particles in suspension by filtration takes place in two steps: transport and attachment (23). For a filter to be effective in removing particles, the particles must be transported to the filter grain surface and then they must be attached to the surface. Transport mechanisms are affected mainly by physical parameters. Attachment of particles on the filter media grains is affected mainly by the surface chemistry of the system, which depends on the pH, ionic strength and type of ionic species in the system. Beneficial changes in the surface characteristics of the filter media and the particles can be brought about by the addition of filter aids.

Ives and Sholji (25) performed experiments using particulate microspheres (diameter 1.3 microns and density 1.4 g/cm^3) and filter media of various sizes. They related the initial filter coefficient to the media size, filtration rate and viscosity of the water without considering capture mechanisms.

$$\lambda_o \propto \frac{1}{DV\mu^2} \tag{29}$$

where

D = filter grain size

V = filtration rate

μ = dynamic viscosity of water.

Ison and Ives (17) derived a functional relationship for filtration by means of dimensional analysis using the Buckingham Π Theorem. They tested their mathematical model using data obtained in a series of experiments using kaolinite suspensions and a bed of nearly monosized glass beads. Three dimensionless groups were used in their statistical analysis: the Reynolds number, a relative size group and a sedimentation group. The resulting functional relation had the form:

$$\Lambda = \text{const}\left(\frac{\rho VD}{\mu}\right)^{-2.7}\left(\frac{d}{D}\right)^{-2.3}\left(\frac{(\rho_s - \rho)d^2 g}{18\mu V}\right)^{1.3} \qquad (30)$$

where

Λ = the fraction of suspension retained in a filter layer one grain diameter thick

ρ = density of fluid

ρ_s = density of the suspended solids particle

d = the effective diameter of the suspended solids particle

g = the gravitational constant.

Equation 30 was reduced to

$$\lambda_o = \frac{\Lambda}{D} = \text{const}\frac{\mu^{1.4}\, d^{0.3}}{D^{1.4}\, v^4}$$

Their results illustrated the importance of the gravitational forces on suspensions whose particle density is appreciably greater than the suspending phase and the influence of the Reynolds number on the removal.

Heertjes and Lerk (14) assumed that forces acting on iron hydroxide particles are only the London-van der Waals forces and the Stokes drag force. Their filter coefficient was:

$$\lambda = \text{const}\ \frac{(1 - \epsilon_o)Q}{\mu D_o^3 V}$$

where

Q = the Hamaker constant

D_o = the initial mean particle diameter of the filter material

μ = the viscosity of the fluid.

Mackrle and Mackrle (31) also derived a relationship based on the London-van der Waals forces, the Stokes drag force and the Reynolds number for the filtration of iron hydroxide and aluminum hydroxide suspensions. According to their experimental results,

$$\lambda_o \propto \frac{\mu}{d^2 V}$$

Ives (20) indicated that the van der Waals forces could contribute to attachment but he did not feel that these forces were a dominant part of the mechanism that could be used in the derivation of a kinetic equation because the van der Waals forces are only significant at very close range (less than 0.1 micron).

Ives (21) obtained a filter efficiency equation by combining the significant transport mechanisms in filtration: interception, diffusion, sedimentation and hydrodynamic effects.

$$\Lambda = \text{const } \left[\frac{d}{D}\right]^{\alpha} \left[\frac{kT}{3\pi\mu dVD}\right]^{\beta} \left[\frac{g(\rho_s - \rho)d^2}{18\mu V}\right]^{\gamma} \left[\frac{\mu}{\rho DV}\right]^{\delta}$$

where

T = the absolute temperature

k = the Boltzmann's constant

and α, β, γ, δ are positive exponents.

Collecting terms gave:

$$\Lambda = \text{const } \frac{d^{\alpha-\beta+2\gamma}}{\mu^{\beta+\gamma+\delta} D^{\alpha+\beta+\delta} V^{\beta+\gamma+\delta}} (kT)^{\beta} (\rho_s - \rho)^{\gamma} \rho^{-\delta} \qquad (31)$$

By determining the value of α, β, γ and δ, it is possible

to determine the relative importance of the four mechanisms in the filtration of a particular suspension.

Some investigators have considered attachment mechnisms as well as transport mechanisms. The main forces which affect the attachment of particles on the filter grain surface are van der Waals forces (attraction) and electric double-layer interactions (either attraction or repulsion). The range of surface forces are extremely limited, so the combined effects of these forces will only give a favorable condition or provide a barrier for the attachment. In the favorable condition, there would be no more improvement in filtration efficiency as was illustrated for the case of the single spherical collector model by Rajagopalan and Tien (41).

Ghosh et al. (11) showed the dependence of the initial filter coefficient on filtration rate for the filtration of latex microspheres. For systems where the effects of gravity and double-layer repulsion were insignificant, the initial filter coefficient varied as the -1.8 to -2.0 power of the approach velocity at higher rates of filtration ($v > 0.1$ cm/s) and as the -0.67 to -1.0 power of the approach velocity at lower rates of filtration ($v < 0.1$ cm/s). For the systems where the effect of gravity was negligible, and the effects of double-layer repulsion were significant, the coefficient varied as the -0.43 to -1.0 power of the approach velocity at

higher filtration rates and as -0.3 to -0.55 at lower filtration rates.

In each of the models, a number of transport mechanisms may operate simultaneously. The relative significance of each mechanism depends on the nature of the suspension as well as the operation of the filter. Therefore, the filtration coefficient can vary widely depending on both chemical and physical conditions that exist during a filter run.

Trajectory Model

Some investigators tried to estimate the rate of particle deposition by a trajectory analyses of particle motion. The idea of using particle trajectories to compute capture efficiency was introduced in aerosol filtration studies more than 40 years ago. O'Melia and Stumm (36) suggested its use in water filtration. Shortly thereafter Yao, Habibian and O'Melia (58) calculated the filter coefficient based on the single sphere collector efficiency. They considered the combined effects of diffusion, interception and gravity.

For the development of a trajectory model, a granular filter bed was viewed to be an assembly of particle collectors. Any model which adequately describes the flow

field can be used, but the complexity of the actual situation necessitated some form of simplification. The models employed by various investigators can be grouped into three categories: capillary collectors, spherical collectors and constricted tube collectors. Particle trajectories around a collector are obtained from the integration of the appropriate equations of particle motion, which are obtained from the balance of forces and torques acting on the particle. The forces are gravity, hydrodynamic drag and surface forces. The effect of interception is included as a boundary condition. The contribution from Brownian diffusion is added to the capture by trajectory analysis in determining the overall capture. Generally, these equations were solved numerically and collector efficiency was correlated with relevant dimensionless parameters. Finally, the filter coefficient, λ, was obtained from calculations based on the unit collector efficiency and was used in Equation 1 (40,55).

Spielman and Fitzpatrick (48) incorporated gravitational, hydrodynamic and London-van der Waals forces simultaneously in developing trajectory equations for the motion of nondiffusing particles where double layer forces were negligible. Numerical solutions were used to determine the initial filter coefficient. The curves that they published were dimensionless plots based on the functional relationship:

$$\lambda_o = \lambda_{oi}\, f(N_{Ad}, N_{Gr}) \qquad (32)$$

where

λ_{oi} = filter coefficient for interception ($9\alpha A_s d^2/D^3$)

α = solids fraction (volume fraction of the grain)

A_s = a parameter characteristics of flow model

N_{Ad} = an adhesion group based on a spherical filter grain ($QD^2/9\pi\mu A_s V d^4$)

N_{Gr} = a gravitational group based on a spherical filter grain ($2(\rho_s - \rho)gD^2/9\pi A_s V$)

Q = the Hamaker constant.

Fitzpatrick and Spielman (10) measured the initial (clean bed) removal of a latex suspension through beds of glass beads and compared their results to the predicted results based on their model. They summarized both the experimentally observed and theoretically predicted ranges of the filter coefficient as it was affected by the particle diameter, grain diameter, filtration rate, porosity and Hamaker constant. Their results are shown in Table 1. The initial filter coefficient was expressed as:

$$\lambda_o = d^a Q^f / D^b V^c \alpha^e \qquad (33)$$

Table 1. Fitzpatrick and Spielman's comparison of theoretical and observed values of the filter coefficient[a] (10)

Exponent	Approx. range of exponent			
	Theory[b]		Experiment	
	$N_{Gr} = 0$	$N_{Gr} >> 1$	$N_{Gr} < 1.0$	$N_{Gr} \geq 10.0$
a	1.2-0.67[c]	2.0	1.0	1.8-2.2[d]
b	2.6-2.3	1.3-0.0	1.7-2.3[e]	——
c	0.1-0.3	0.3-1.0	0.1-0.5[e]	1.0[d]
e	2.5-1.3	2.5-1.3	——	——
f	0.1-0.3	0.3-0.0	——	——

[a] $\lambda_o = d^a Q^f / D^b V^c \alpha^e$.

[b] Spielman and Fitzpatrick (48).

[c] The first value of any group corresponds to $N_{Ad} << 1$ and the second corresponds to $N_{Ad} >> 1$.

[d] This range of exponent was observed for all N_{Ad}.

[e] This range of exponent was observed over all $N_{Ad} < 1$.

Predictions of the coefficient were in fairly good agreement with theory at the intermediate filtration rate (0.1 - 0.3 cm/sec), but the variance was fairly large.

In the last ten years, trajectory models have been studied intensively at Syracuse University. Their simulation procedure for predicting the behavior of deep bed filtration has been well-documented (40, 55, 56). They viewed the deposition process as consisting of two stages. In the first stage, a relatively smooth layer of the deposit forms on the filter grain surfaces. In the second stage, particle deposits are lodged at the pore constrictions of the filter bed and thus block the flow of the suspension through these pore spaces. Happel's sphere model was used to describe the initial period of deposition and the constricted tube model for the later stages of deposition. When the specific deposit reaches a critical value, a transition from a smooth coating mode to a blocking mode is assumed to occur. The filter coefficient, λ, increases until the specific deposit reaches the transition value and then decreases. This model is consistent with Ives' hypothesis describing the variation in the filter coefficient. The hypothesis proposed by the Syracuse group is that deposition ceases when the interstitial velocity exceeds a critical value in accordance with Maroudas and Eisenklam's model. The Carman-Kozeny equation was used to estimate the head loss through the

filter bed during the first stage of deposition and the pressure drop was estimated by the number of unit cells still available for flow during the second stage.

They considered gravity, London-van der Waals attraction, double layer interactions, drag and particle inertia in deriving their trajectory equations. Diffusive transport was added to the results of the trajectory calculations. The initial filter coefficient that they derived (40) was:

$$\lambda = 1.08(1 - \epsilon_o)A_s N_{LO}^{1/8} N_R^{15/8} + 3.6\times10^{-3}(1 - \epsilon_o)A_s N_G^{1.2} N_R^{-0.4} + 6(1 - \epsilon_o)A_s^{1/3} N_{Pe}^{-2/3} \quad (34)$$

where

N_{LO} = the London group $(Q/9\pi\mu d^2 V)$

N_R = a relative size group (d/D)

N_G = a gravity group $(2d^2(\rho_s - \rho)g/9\mu V)$

N_{Pe} = the Peclet number $(6\pi\mu dDV/kT)$.

As filtration proceeds, the filter coefficient is modified by considering the changes of deposition morphology, bed porosity, grain size and interstitial velocity.

Even though they used a very fundamental approach by applying the removal mechanisms to derive the trajectory of a particle, significant discrepancies still exist between the expected and experimental results. This may be due to the fact that they used a single collector as a representative element to estimate the filter efficiency even though contact between the individual grains violates the concept of a single collector model. These questions about the soundness of the trajectory model have been expressed by Spielman (47). Still, the trajectory model provides a useful approach to understanding the removal mechanisms and the effects of important variables on filtration.

Head Loss Equation

Some investigators have proposed purely empirical formulas to represent the influence of the specific deposit (retention), σ, on the pressure drop through a filter. Most of these formulas (15) may be written as:

$$\frac{\Delta P}{(\Delta P)_o} = \frac{1}{(1 - j\sigma)^m} \tag{35}$$

where

ΔP = the pressure drop through an element of thickness Δx

$(\Delta P)_o$ = the pressure drop across a thickness, Δx, of a clean porous bed

and where j and m are constants.

Expanding Equation 35 when $j\sigma$ is small:

$$\frac{\Delta P}{(\Delta P)_o} = 1 + mj\sigma + \frac{m(m+1)}{2} j^2\sigma^2 + \cdots\cdots$$

Ives (19), and Heertjes and Lerk (14) used an equation for head loss per unit depth that applies if $\sigma << \epsilon_o$:

$$\frac{\Delta P}{(\Delta P)_o} = 1 + mj\sigma \qquad (36)$$

Based on equation 36, Ives (19) formulated the following total head loss equation:

$$H = h_o L + \int_0^L k\sigma \, dx \qquad (37)$$

where

h_o = the clean filter hydraulic gradient

k = a constant

L = the filter depth

He substituted for σ the analytic solution from the kinetic equation and the material balance equation to get the total head loss.

Heertjes and Lerk (14) found experimentally that pressure drop through a filter bed increased linearly with the amount of solids filtered. They described the pressure drop by the following equation which is identical with Equation 37.

$$\Delta P = (\Delta P)_o L + \alpha \int_0^L \sigma \, dx \tag{38}$$

They integrated this equation by substituting for σ an analytical solution, Equation 20, so that Equation 38 becomes:

$$\Delta P = (\Delta P)_o L - \alpha \epsilon_o L$$

$$- \frac{\alpha}{K} \ln \left[1 + \exp\left(-VC_o Kt\right) + \exp\left(K\epsilon_o L\right) - 1\right]$$

Head loss through a filter bed in the domain of laminar flow can be predicted by using the fundamental Kozeny-Carman (15) expression:

$$\frac{\partial P}{\partial x} = h_k \frac{\mu V S^2}{\epsilon^3} \tag{39}$$

where

h_k = the Kozeny constant

S = specific surface of the bed

ϵ = porosity of the bed.

As filtration proceeds, the Kozeny constant, h_k, specific surface, S, and porosity, ϵ, need to be modified due to the growth of the deposit. Cleasby and Baumann (8) found that the head loss during filtration was directly proportional to the filtration rate through a clogged bed for filtration rates up to 4 gpm/ft^2. This is indicative of laminar flow conditions and provides a basis for using Equation 39 for the prediction of pressure drop through a clogged bed. Various attempts (6,9,20,39) to predict the head loss development during filtration have been tried using Equation 39.

Sakthivadivel et al. (45) compared a number of equations previously developed from the Kozeny-Carman equation for the prediction of head loss in filtration. They concluded that the various equations differed from each other because of the simplifying assumptions that had been made in each regarding the mode of deposition of particles on the grains, and because of the insufficient knowledge that was available at that time regarding the changes occurring in the shape and tortuosity of the pores during filtration. The various equations proposed on the basis of Kozeny-Carman equation did not give any more information than others that are purely empirical equations.

Tchobanoglous and Eliassen (53) claimed that there are complexities and difficulties associated with using the modified Kozeny-Carman equations that are hard to overcome. Therefore, they have proposed an empirical formula, derived from data that they obtained in the filtration of treated sewage effluent:

$$h = aq^b \tag{40}$$

where

q = the quantity of suspended solids deposited in a filter section

and where a and b are constants.

MODELS FOR THE STUDY

Breakthrough Curve Equation

In the literature review section, kinetic equations and mass balance equations used previously to describe filtration were reviewed. In general, the material balance equations had a similar form, but the kinetic equations were quite different. As discussed in the literature review, it may not be necessary to include a detachment term in the kinetic expression. Adin and Rebhun (2), Saatci (42), and Saleh (46) developed kinetic equations based on a monolayer adsorption model using limited growth concept. Their equations may not be adequate for filtration, however, in monolayer adsorption, surface area becomes the adsorptive capacity and reaction rate will be proportional to the residual capacity. In filtration, layers of particles that collect on the grain surface reduce the volume of pore space but do not necessarily prevent further deposition unless the deposit grows together. This is analogous to multilayer adsorption.

From the trajectory analyses, the filter coefficient could be given in terms of dimensionless groups:

$$\lambda = f(N_{Lo}, N_R, N_G, N_{Pe}, N_{Dl}) \tag{41}$$

where

N_{Dl} = a zeta potential group ($3D_i d \zeta_p \zeta_s / 2Q$)

D_i = the dielectric constant

ζ_p = the zeta potential of the particles

ζ_s = the zeta potential of the filter grains.

Equation 41 can be rewritten as follows by using all the variables:

$$\lambda = f(d, D, V, \zeta_p, \zeta_s, \rho, \rho_s, \mu, T)$$

where ρ and μ are functions of T. Therefore:

$$\lambda = f(d, D, V, \zeta_p, \zeta_s, \rho_s, T)$$

D is based on the filter grains, and d and ρ_s are based on the suspensions. The zeta potentials of the particles and the filter grains, ζ_p and ζ_s, depend on chemical factors such as pH, ionic strength and ionic species in the system and are modified by the use of filter aids. Therefore, at a given temperature, with a given suspension, filter medum and pretreatment method, the filter coefficient would be primarily dependent on the filtration rate.

The particle removal rate will be proportional to the

active surface area available for the attachment of suspended solids to the filter media grains. Change of interstitial velocity due to the deposit of particles in the flow path will also affect the removal efficiency. Therefore,

$$\frac{\partial \sigma}{\partial t} = \text{const x (surface area per unit filter volume)} \\ \text{x (No. of particles per unit surface area)} \\ \text{x (velocity terms)} \qquad (42)$$

The surface area of the media varies throughout the filtration run and the number of particles per unit of surface area varies during the filter run. Since the product of these two terms must be constant, the deposition rate of particles should be a function of the filtration rate only.

Maroudas and Eisenklam (32), using both theoretical and experimental studies, showed that the nonretaining stage at which no deposition took place could be characterized by a critical interstitial velocity. They indicated that the filter coefficient would be proportional to the difference between the reciprocals of the interstitial and critical velocities as shown by Equation 12. More generally the filter coefficient could be obtained by assuming that it is proportional to some power, x, of the difference (20):

$$\lambda = \text{const} \left[\frac{1}{u} - \frac{1}{u_c}\right]^x$$

For a particular suspension,

$$\lambda = \text{const} \left[\frac{\sigma_u - \sigma}{V}\right]^x \tag{43}$$

where

x = constant

σ, σ_u = the deposit volume and the ultimate deposit volume per unit of filter volume.

Then the kinetic equation, Equation 6 becomes:

$$\frac{\partial \sigma}{\partial t} = \text{const} \left(\frac{\sigma_u - \sigma}{V}\right)^x VC \tag{44}$$

The value of x can be estimated if the mechanisms involved in the filtration process are known. In general, an estimated filtration coefficient from theory is likely to be quite different from the actual one. The arbitrary power, x, complicates the process of solving the kinetic equation and the material balance equation. If x were equal to one, the solution is easily obtained. Then, the kinetic equation becomes:

$$\frac{\partial \sigma}{\partial t} = K(\sigma_u - \sigma)C \tag{45}$$

This is identical to the limited growth model and has the

same form as Saatci's kinetic equation in which the detachment term was neglected. Equation 2 is a mass balance equation which neglects the particulates in the void spaces between the grains:

$$\frac{\partial \sigma}{\partial t} + V \frac{\partial C}{\partial x} = 0 \qquad (2)$$

Based on these equations, a solution can be easily obtained for C and σ as a function of service time, t, and filter depth, x, for a given influent suspended solids concentration, C_o, and filtration rate, V, as shown in the Appendix:

$$C = \frac{C_o}{\exp\ (Kx\sigma_u/V - KC_o t) - \exp\ (-KC_o t) + 1} \qquad (46)$$

$$\sigma = \frac{\sigma_u [1 - \exp\ (-KC_o t)]}{\exp\ (Kx\sigma_u/V - KC_o t) - \exp\ (-KC_o t) + 1} \qquad (47)$$

Therefore, it may be practical to use 1 as the value of x and let the constant become a function of filtration rate and $\sigma_u - \sigma$. This may have the effect, however, of restricting the range over which the resulting equations apply. Rearranging Equation 46 as shown in the Appendix:

$$-\ln\ (C_o/C - 1) = -\ln\ [\exp\ (Kxo_u/V) - 1] + KC_o t \qquad (48)$$

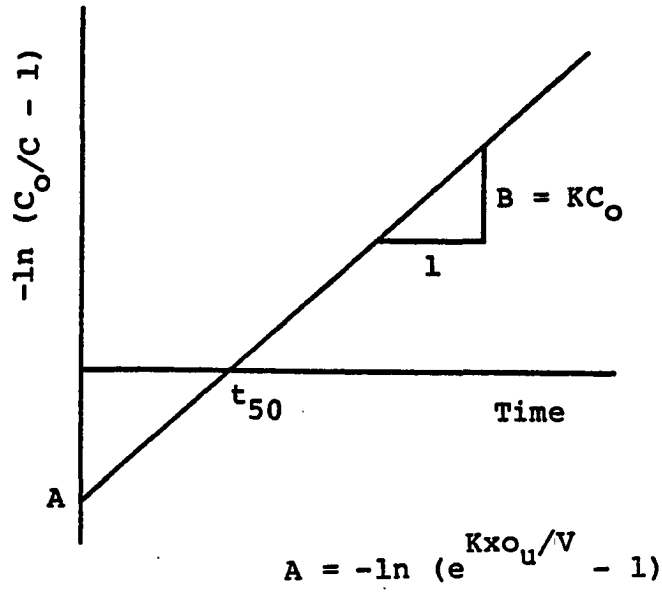

Figure 2. Linear transformation of C/C_o versus t

According to Equation 48, data from a filtration run can be linearized by plotting $-\ln (C_o/C - 1)$ versus t (Figure 2). The slope of the regression line, B, may be used to estimate the value of the attachment coefficient, K:

$$K = \frac{B}{C_o} \tag{49}$$

The intercept on the $-\ln (c_o/C - 1)$ axis, A, can be used in estimating the value of the filter capacity, σ_u:

$$\sigma_u = \frac{V}{K\bar{x}} \ln (e^{-A} + 1) \qquad (50)$$

Head Loss Equation

To apply modified forms of the Kozeny-Carman model, many simplifying assumptions must be made regarding the mode of deposition of particles on the filter grain surface, and the shape and tortuosity of the pores during filtration. This may be the reason why formulations based on the Kozeny-Carman equation do not give any better prediction than the purely empirical expressions.

Therefore, an empirical formula for the prediction of head loss will be outlined in this section. The first assumption that will be made is that the head loss per unit depth is proportional to the local specific deposit.

$$\frac{\partial H}{\partial x} = \left(\frac{\partial H}{\partial x}\right)_o + a\sigma \qquad (51)$$

where a is constant.

Integration of Equation 51 with respect to the filter depth, L, gives the total head loss through that depth.

$$H = \int_0^L \left(\frac{\partial H}{\partial x}\right)_o dx + \int_0^L a\sigma \, dx$$

$$H = H_o + a\int_0^L \sigma \, dx$$

The integral, $\int_0^L \sigma \, dx$, denotes the total deposits in the filter. It can be integrated as shown in the Appendix by inserting Equation 47 in place of σ which represents the local specific deposit. The total deposits in the filter also can be estimated by the difference between the total incoming and outgoing solids up to a given time, but that would be much more tedious. Using Equation 47 in place of σ:

$$H = H_o + a\left[\sigma_u L - \frac{V}{K} \ln \left[\exp\left(KC_o t\right) + \exp\left(K\sigma_u L/V\right) - 1\right] + C_o V t\right] \qquad (52)$$

From the observations of filter runs, head loss increases continuously even though effluent quality is degraded. The growth rate of the specific deposit decreases as the effluent quality degrades. Therefore, it may be assumed that the head loss increases geometrically with respect to the specific deposit as Tchobanoglous and Eliassen observed (53). Equation 52 may be modified as follows:

$$H = H_o + a\left[\sigma_u L - \frac{V}{K} \ln \left[\exp\left(KC_o t\right) + \exp\left(K\sigma_u L/V\right) - 1\right] + C_o V t\right]^b \qquad (53)$$

The constants, a and b, can be determined by regression analysis using the head loss data from a filtration run.

EXPERIMENTAL INVESTIGATION

To accomplish the objectives of this study, breakthrough curves for different influent suspended solids concentrations, filtration rates, media sizes and depths were needed. To restrict the scope of the investigation, the research was limited to hydrous ferric oxide suspensions. Hydrous ferric oxide suspensions were prepared by adding a 0.2 M ferrous sulphate stock solution to the university tap water in a mixing tank.

Oxidation of Fe(II) to Fe(III)

The university tap water has been softened to a total hardness of about 140 to 165 mg/l as $CaCO_3$ and the total alkalinity is about 30 to 40 mg/l. Stumm and Lee (51) described the oxidation of iron(II) in bicarbonate solutions in the neutral pH range by the following equation:

$$\frac{d[Fe^{++}]}{dt} = -k[P_{O_2}] [OH^-]^2 [Fe^{++}] \qquad (54)$$

where

$\frac{d[Fe^{++}]}{dt}$ = the rate of iron (II) oxidation (moles/liter-min)

k = a reaction rate constant (about 8×10^{13} liter^2/mole^2-atm-min at 20.5°C)

P_{O_2} = the partial pressure of oxygen in the gas phase (about 0.21 atm)

$[OH^-]$ = the hydroxide ion concentration (moles/l)

$[Fe^{++}]$ = the iron(II) concentration (moles/l).

An expression for the apparent reaction rate constant, K_{app}, has been used (4) to eliminate the actual rate constant, k:

$$K_{app} = k[P_{O_2}]\ Kw^2/[H^+]^2 \tag{55}$$

Thus, Equation 54 becomes:

$$\frac{d[Fe^{++}]}{dt} = -K_{app}[Fe^{++}] \tag{56}$$

From Equation 55, it may be interpreted that an increase in solution pH results in an increase in the rate of oxidation.

According to Ghosh (37), the activation energy (E_a) for this reaction is 23 K calories per mole, therefore:

$$\ln\ (k_1/k_2) = \frac{E_a(T_2 - T_1)}{RT_2T_1} \tag{57}$$

where

R = the gas law constant (1.98 cal/degree-mole)

T_1, T_2 = the absolute temperature in ^{o}K.

In a completely mixed flow reactor, the required detention time to lower the concentration of iron from C_o to C will be given by (29):

$$t = (C_o/C - 1) \frac{1}{K_{app}} \qquad (58)$$

For a detention time of 30 minutes at 18°C and at a pH of 8, $K_{app} = 2.64\ min^{-1}$ from Equations 55 and 57. From Equation 58:

$$C/C_o = 1/(K_{app}t + 1) = 0.0125$$

Thus, the suspension would have about 1% of iron(II) at pH 8 and 18°C. The minimum solubility of $Fe(OH)_3$ in the $Fe(OH)_3$-H_2O system occurs between pH 7 and pH 10 (37). Therefore, the pH of the test suspension was maintained at a value of about pH 8 during the runs. The range in pH was from about 7.5 to 8.6 based on a single reading in each run.

Pilot Plant Apparatus

The pilot plant that was used consisted of a mixing tank, chemical dosing apparatus and five filter columns with

valves, sampling taps and flow meters. Piezometers were connected at the top and bottom of each filter to measure the head loss through the filter bed. The components of the pilot plant are shown in Figure 3.

Mixing tank and chemical dosing apparatus

The rate of incoming tap water was 4.51 gpm into the mixing tank. The mixing tank was 3 ft high, 3 ft in diameter and had 4.5 inches of freeboard. This provided a 30 minute detention time to complete the formation of hydrous ferric oxide floc. An electric motor connected to a reduction gear was used to drive a mixing paddle at 50 rpm. The mixing facilitated the formation of floc.

A 0.2 M ferrous sulphate stock solution which was 0.1 N in sulphuric acid was fed by a capillary tube feeder into the mixing tank. The flow meter (Brooks model 1355) was used to determine the flow rate. The flow rate was adjusted by using a hose clamp to restrict the flow through the feed line and by adjusting the level of the capillary tube feeder. A chemical feed pump (Masterflex model 7565) was used to supply a sodium bicarbonate stock solution used in maintaining the pH of the suspension.

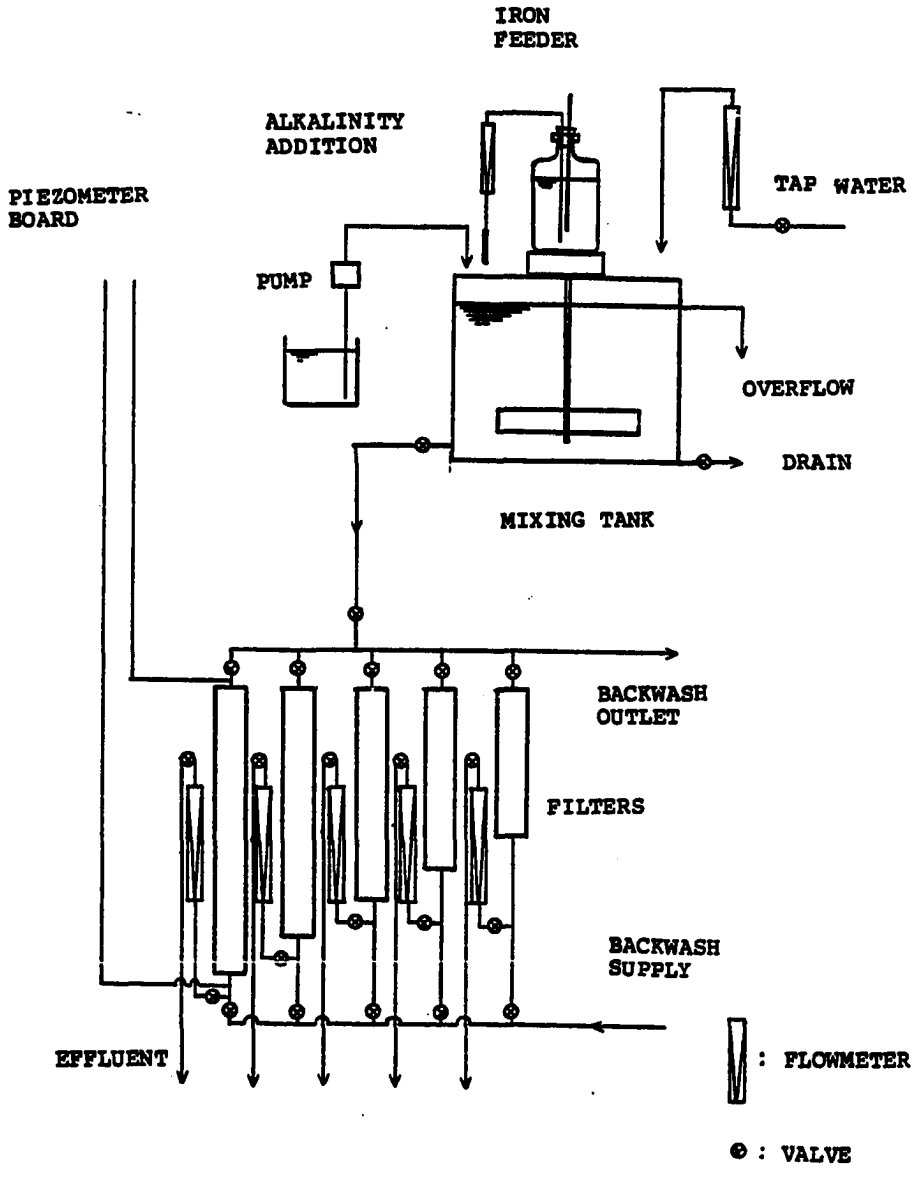

Figure 3. Schematic diagram of experimental filtration system

Filter columns

Five filter columns previously constructed were operated in parallel to investigate the effects of filtration rate and media size on filter performance. The filter columns consisted of 3 inch I.D. Plexiglas columns. A media depth of 10 inches was used for the first six runs; 18 inches for the next nine runs; and varying depths for the last two runs. For identification purposes the filters will be referred to as Filters A, B, C, D, and E. The media in Filter A was prepared by mixing 14 x 16 mesh Muscatine (Iowa) sand (passes a U.S. standard sieve No. 14 and is retained on a U.S. standard sieve No. 16), and 16 x 18 mesh Muscatine sand at the ratio of one to one by weight. For Filters B, C, and D, 18 x 20 and 20 x 25 mesh Muscatine sand were mixed in the same ratio. A 25 x 30 and a 30 x 35 mesh sand were mixed in the same mixing ratio for use in Filter E. Therefore, the mean diameter of the filter media was 1.19 mm for Filter A, 0.841 mm for Filters B, C, and D, and 0.595 mm for Filter E.

Experimental Procedure

Suspension preparation

The 0.2 M ferrous sulphate stock solution was prepared by dissolving ferrous sulphate in distilled water. Each

liter of solution contained 55.6 g of ferrous sulphate and was 0.1 N in sulphuric acid. The stock solution of sodium bicarbonate was prepared by diluting 65 g of sodium bicarbonate to 1 liter using distilled water.

The influent suspension for the filter runs was prepared by adding the stock solutions to the university tap water. The tap water was supplied at the rate of 4.51 gpm. The ferrous sulphate and sodium bicarbonate stock solution were dripping into the mixing tank at controlled rates. Although the paddle on the mixing tank was operated continuously, it was suspected that there could be a buildup of heavy floc near the bottom of the tank if nothing was done to prevent that. Consequently, the bottom drain on the tank was left partially open to provide a continuous removal of suspension from the bottom of the mixing tank.

The university tap water is supplied by the City of Ames. The water is pumped from wells 100 to 130 ft deep and treated by lime softening, filtration, fluoridation and chlorination. During the filtration runs, the pH was about 9.5, the total hardness varied between 140 and 165 mg/l as $CaCO_3$ and the total alkalinity was 30 to 40 mg/l as $CaCO_3$. Variations of water quality at the Ames water treatment plant are shown in Table 2. During any given filter run, the water quality of Ames water supply remained relatively constant.

Table 2. Water quality variations of Ames water supply during the filtration runs[a]

Date	pH[b]	Alkalinity[b] (mg/l as $CaCO_3$)	Hardness[c] (mg/l as $CaCO_3$)	Temperature[b] (^oF)
7/5/1982	9.4	36	146	56
7/10	9.4	33	161	56
7/17	9.4	35	154	56
8/24	9.8	41	153	56
8/28	9.5	36	145	55
9/2	9.4	33	163	56
9/6	9.6	28	156	56
9/11	9.7	33	161	56
9/14	9.6	35	165	56
9/23	9.6	33	162	55
9/25	9.6	33	162	55

[a]From the Ames water treatment plant log.

[b]Plant tap.

[c]Filter effluent.

Table 3. Influent conditions for various filter runs

Run No.	Iron con. (mg/l)	Temperature (^oC)	pH	Alkalinity (mg/l as $CaCO_3$)	Date
3	4.1	17	8.2	110	7/5/1982
6	6.24	18.5	7.9	110	7/17
4	7.59	18	7.6	110	7/10
9	3.95	18.8	8.6	110	8/24
16	3.67	18	8.3	107	9/14
12	5.68	18.5	7.8	110	9/2
15	5.71	19	7.9	105	9/11
10	7.63	18.8	7.7	100	8/28
14	7.42	19	8.0	105	9/6
17	5.95	18.2	7.5	110	9/23
18	5.74	18.2	7.9	105	9/25

Filter conditioning period

To insure that the same initial conditions were maintained from run to run, a conditioning period of 2.5 hours was used. During the conditioning period, the filters were operated at a filtration rate of 6 gpm/ft^2 for a period of 2.5 hours, they were then backwashed and the experimental run was then started immediately.

Filter run

The first six filter runs were made using filters that were 10 inches deep. The data for three of these runs were eliminated because of a variety of operating difficulties. The next nine runs were made using filters that were 18 inches deep. The data from three of these runs were eliminated. Runs were made at 3 different influent iron concentrations, about 4, 6 and 8 mg/l. When the tests on 18 inch depths of filter media were made, two runs were made at each concentration to confirm the reproducibility of the results. Filter A contained sand with a mean diameter of 1.19 mm, Filter C of 0.841 mm and Filter E of 0.595 mm. They were all operated at a filtration rate of 6 gpm/ft^2. Filters B and D with 0.841 mm sand were also operated at filtration rates of 4 and 8 gpm/ft^2. Two more runs with an influent iron concentration of about 6 mg/l and a filtration rate of 6

gpm/ft^2 were made using fiters with a depth of 30 inches.

In general, samples of influent and effluent were taken and head losses through filters were measured at 45-minute intervals. The influent samples were taken from one of the sampling cocks located in the influent line. The effluent samples were obtained at outlet points located beyond each flow meter. Total iron concentrations were measured by the 1,10-phenanthroline method. Ferro Ver Iron Reagent powder pillows (Hach Chemical Company) were used to dissolve and reduce the iron precipitates in a one step work up procedure without heating. A Beckman Model B Spectrometer was used to do the colorimetric measurements. The filters were operated until enough data were collected so that a breakthrough curve could be developed. This represented a ratio of C/C_o ranging from about 0.2 to 0.6.

On completion of a filter run, the filters were backwashed for a period of 15 minutes and the piezometers and flow meters were flushed with tap water to remove iron deposits that accumulated during the filter run.

Results of the Experiments and Application of Models

Influent conditions for the various filter runs are summarized in Table 3. For Runs 6, 9, 10, 12 and 18,

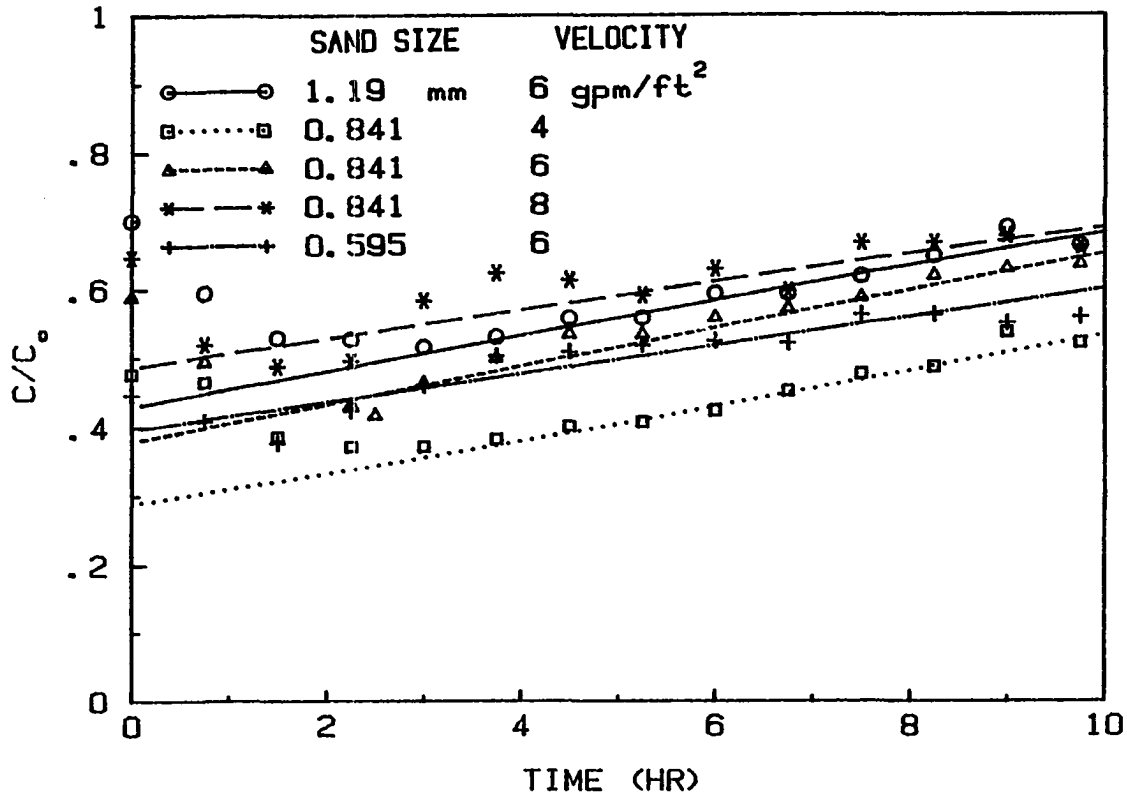

Figure 4. Breakthrough curves of Run 6
(L = 10 in, C_o = 6.24 mg/l)

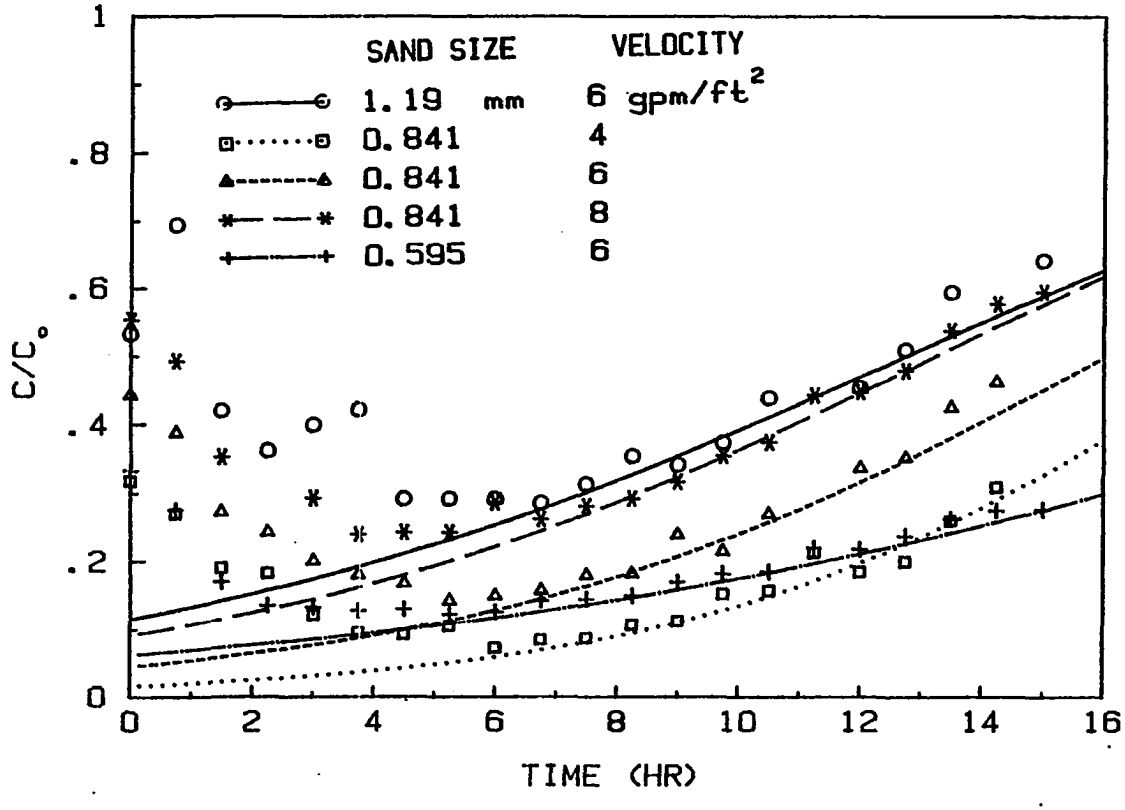

Figure 5. Breakthrough curves of Run 9
(L = 18 in, C_o = 3.95 mg/l)

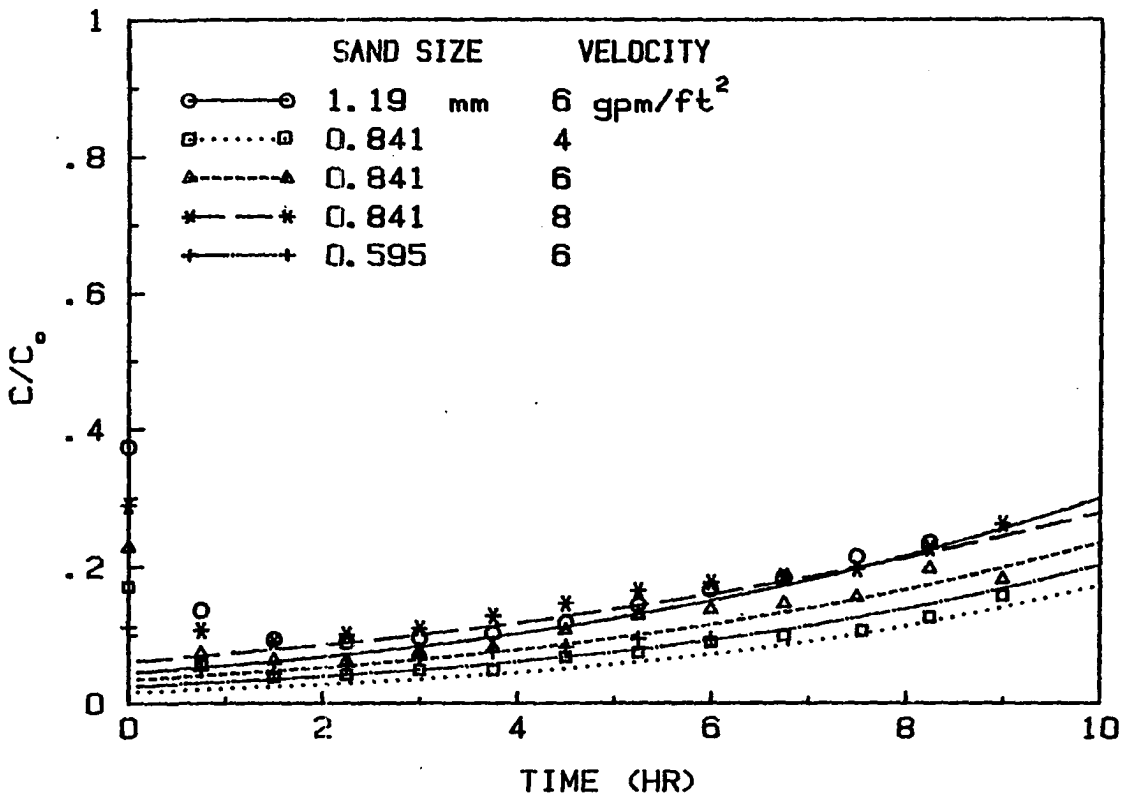

Figure 6. Breakthrough curves of Run 10
(L = 18 in, C_o = 7.63 mg/l)

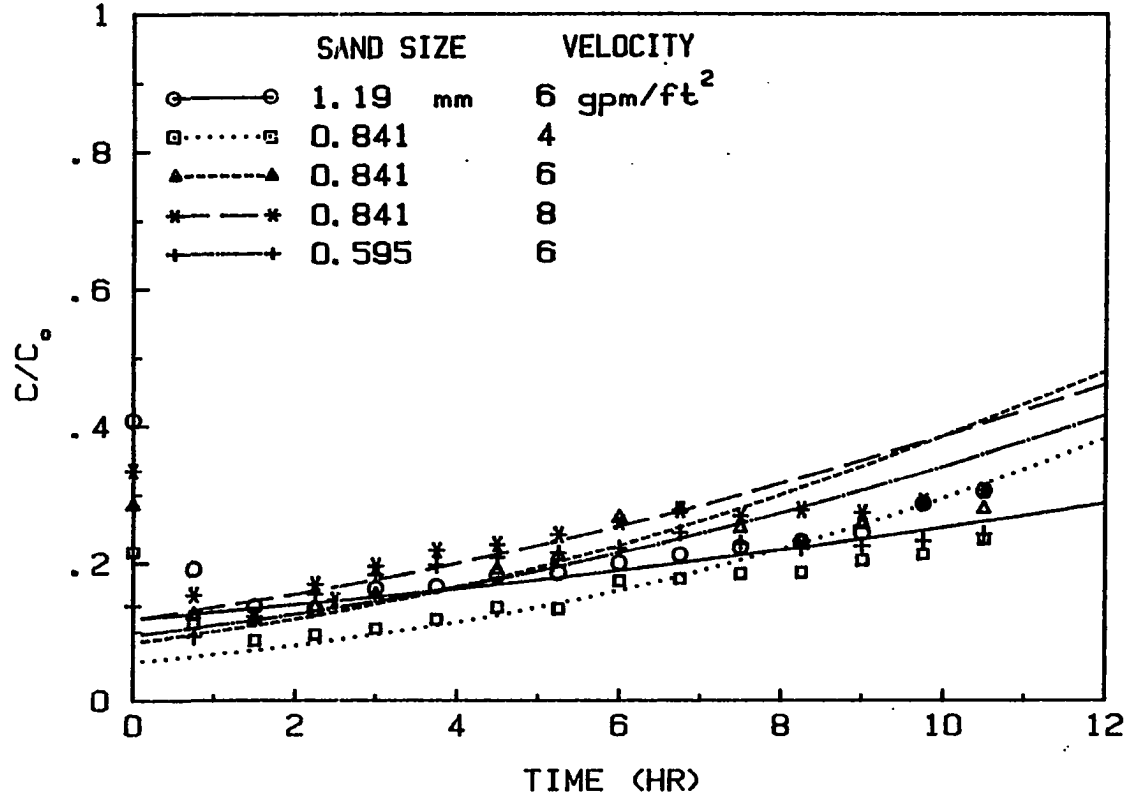

Figure 7. Breakthrough curves of Run 12 (L = 18 in, C_o = 5.68 mg/l)

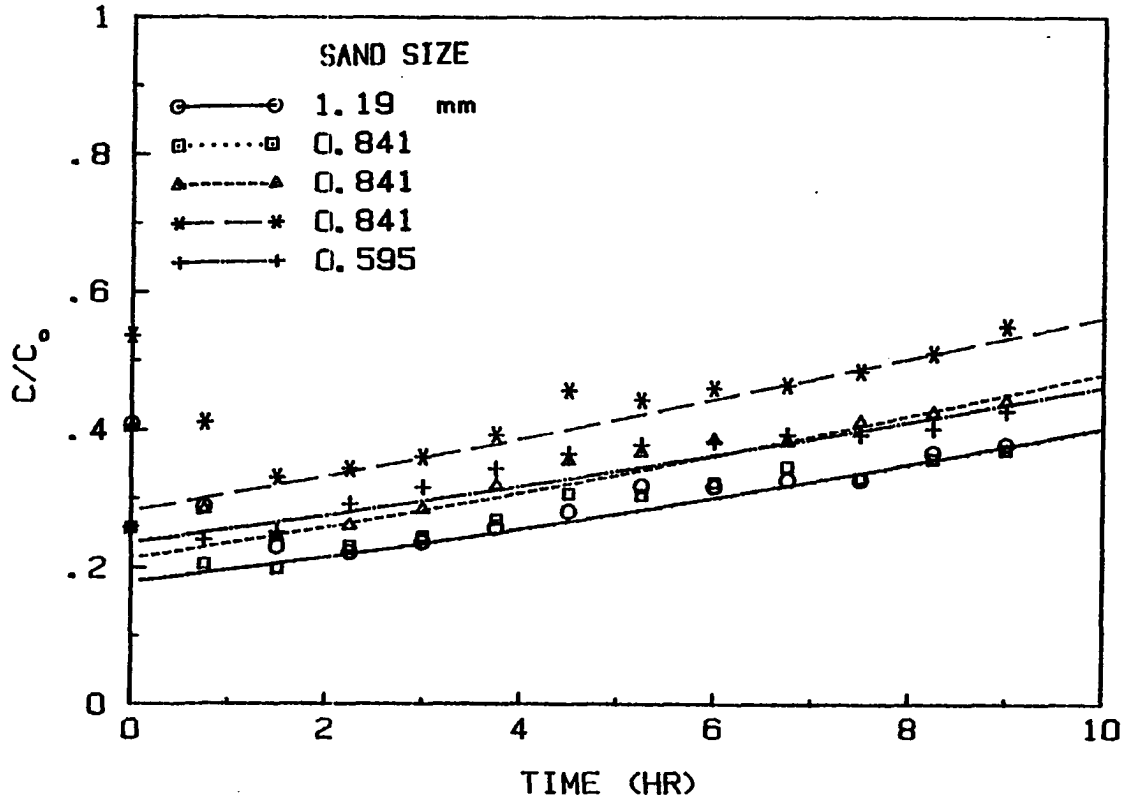

Figure 8. Breakthrough curves of Run 18
(C_o = 5.74 mg/l, V = 6 gpm/ft^2)

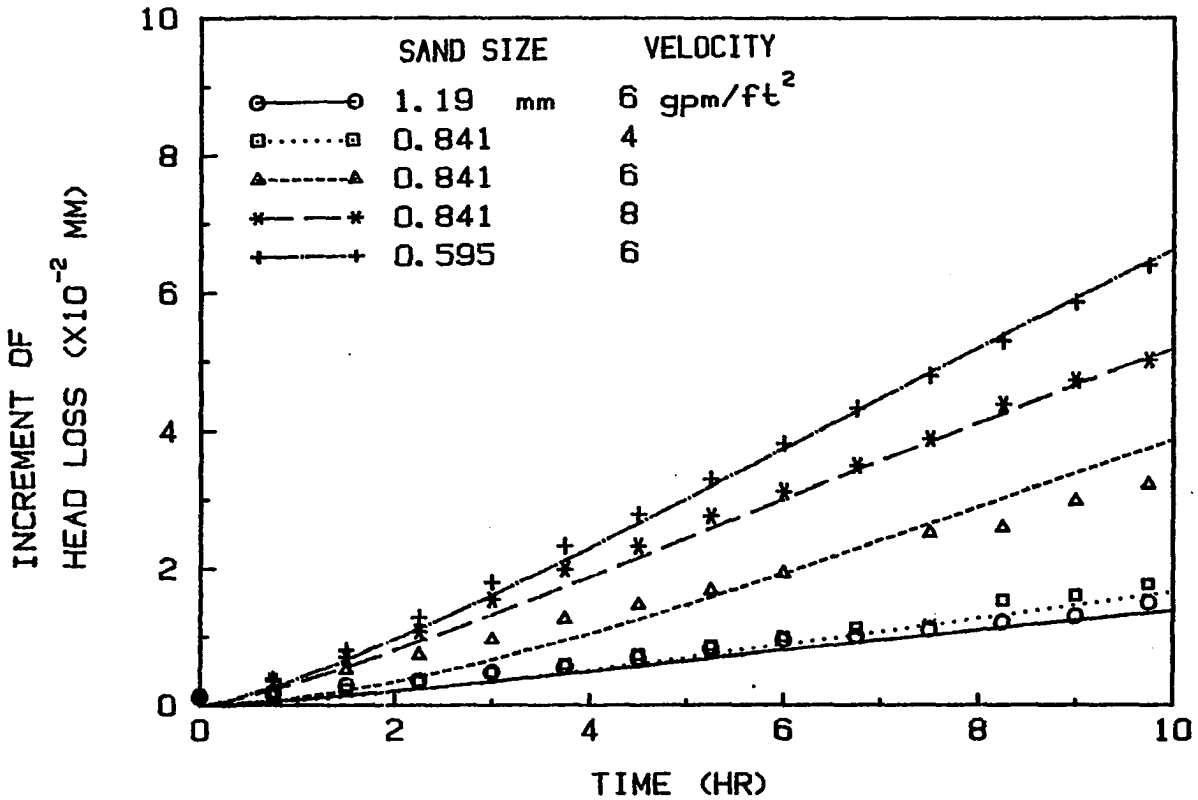

Figure 9. Head loss development curves of Run 6 (L = 10 in, C_o = 6.24 mg/l)

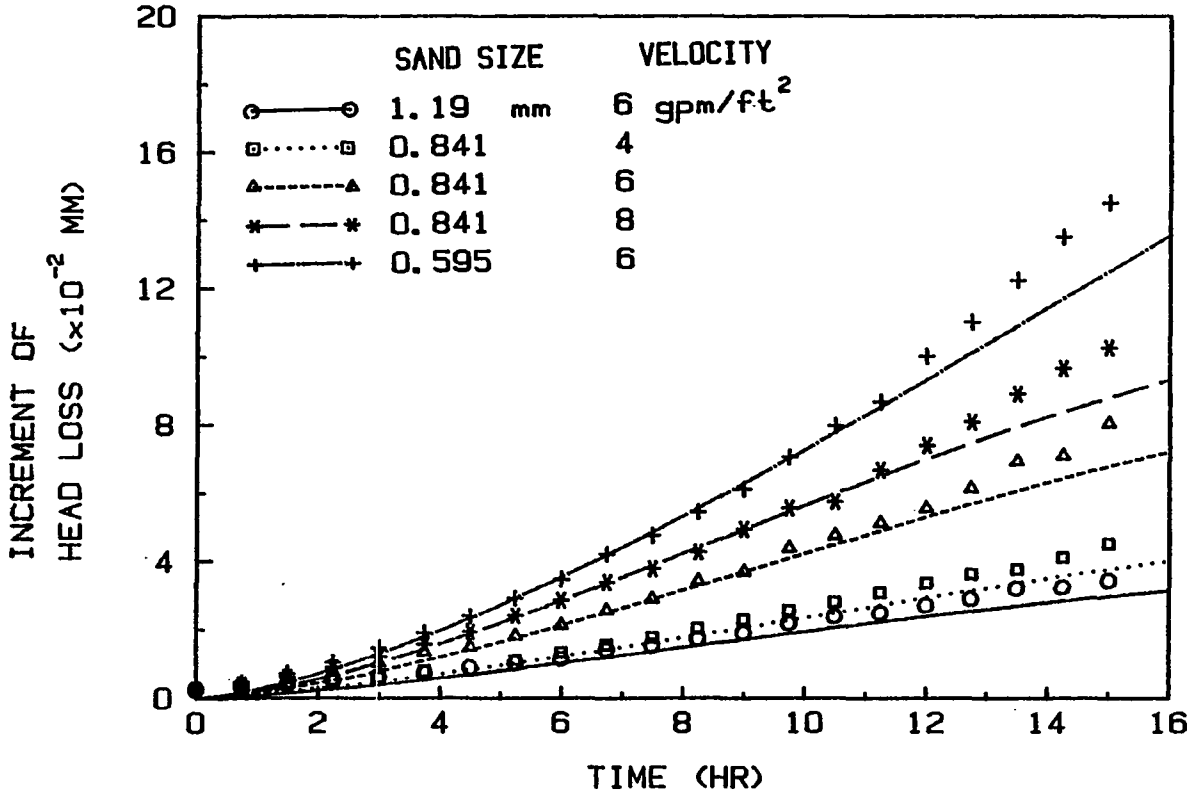

Figure 10. Head loss development curves of Run 9 (L = 18 in, C_o = 3.95 mg/l)

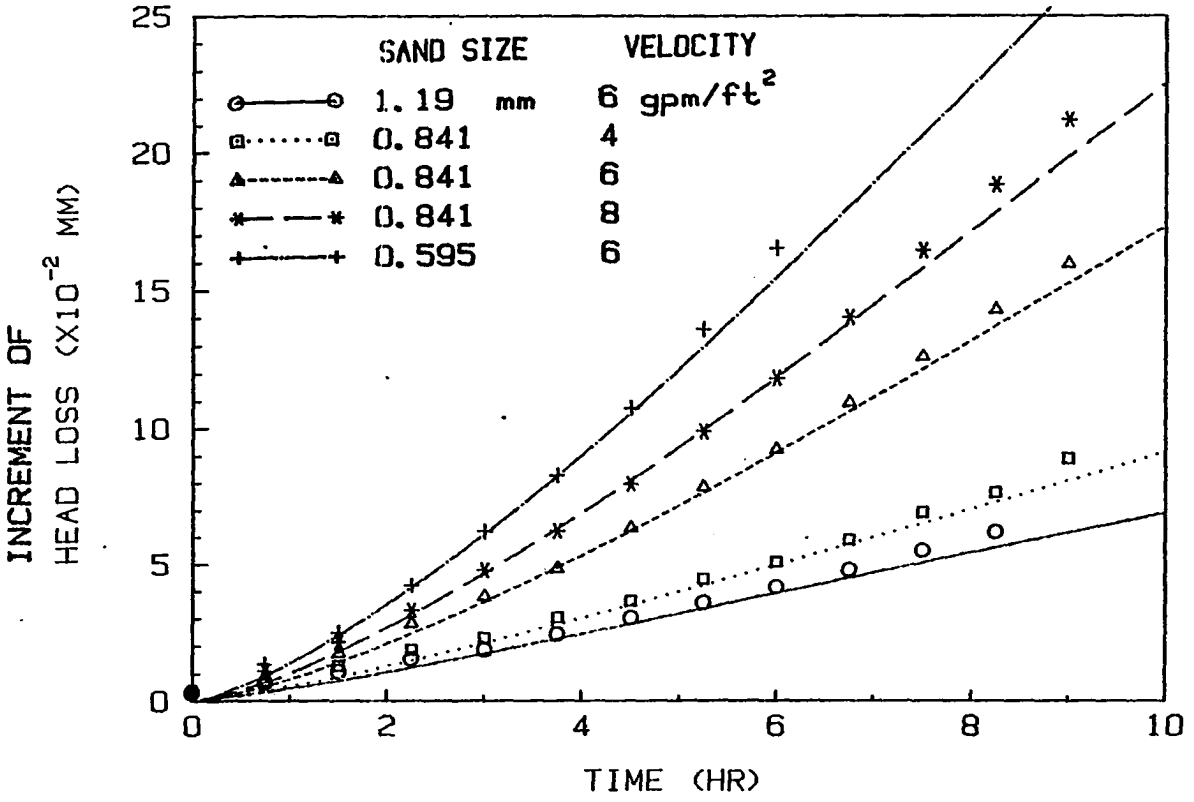

Figure 11. Head loss development curves of Run 10 (L = 18 in, C_o = 7.63 mg/l)

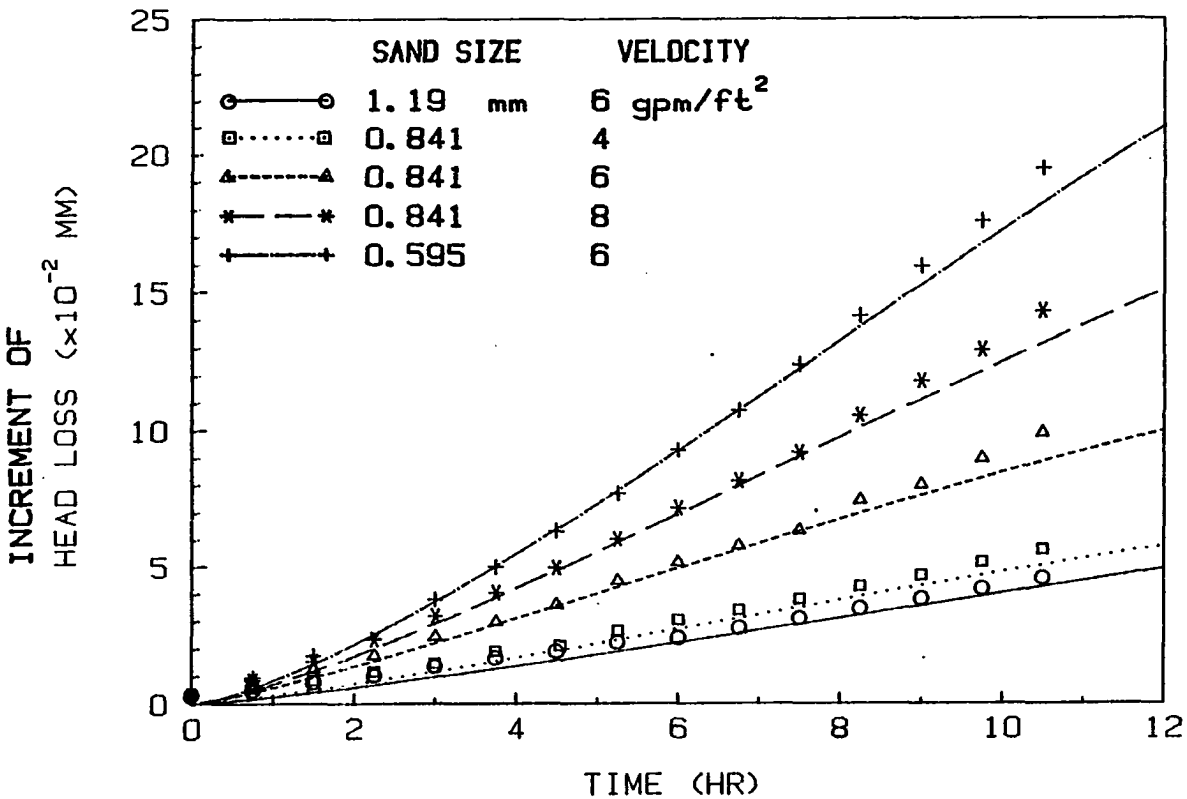

Figure 12. Head loss development curves of Run 12 (L = 18 in, C_o = 5.68 mg/l)

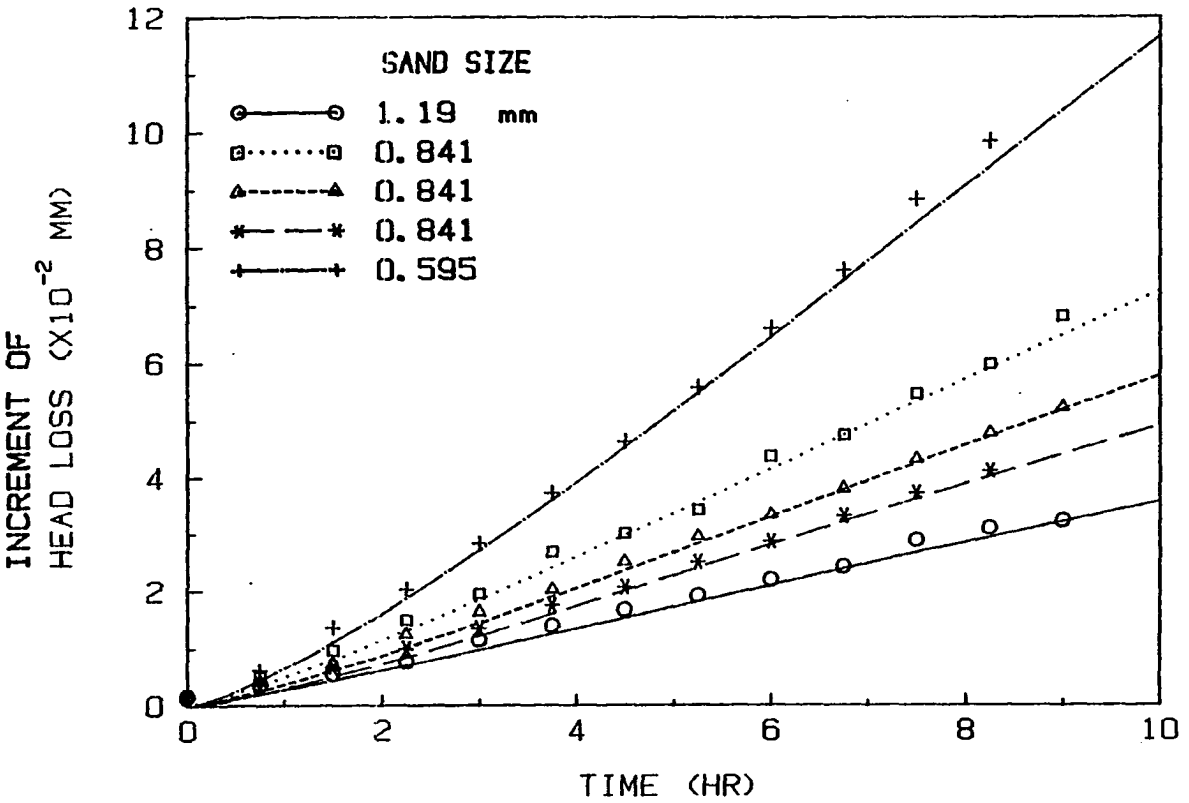

Figure 13. Head loss development curves of Run 18
(C_o = 5.74 mg/l, V = 6 gpm/ft^2)

selected data for the breakthrough curves are plotted in Figures 4-8, and data for the increment of head loss (head loss minus initial head loss) are plotted in Figures 9-13. Using estimated filter coefficients, σ_u and K, and head loss constants, a and b, theoretical breakthrough curves and head loss curves were drawn on those figures.

Calculation of filtration coefficients

The improvement in effluent quality during the filter ripening period can be explained as a phenomenon that is related to events that occur during the backwash stage as was discussed in the literature review section. This improvement in effluent quality cannot be modeled with the relationships that are being developed in this dissertation. Therefore, only the degradation period in which the breakthrough curve rises will be used to determine the filtration coefficients. Corresponding values of $-\ln (c_o/C - 1)$ and t were plotted. The slope and intercept were determined by regression analysis. Then the attachment coefficient, K, and filter capacity, σ_u were calculated by Equations 49 and 50. A woked example and data from the runs using the 18-in filters are shown in the Appendix.

For runs employing a 10-in deep filter, the computed

filtration coefficients, K and σ_u, are summarized in Tables 4 and 5. The attachment coefficient, K, and filter capacity, σ_u, with an 18-in deep filter at 3 different filtration rates (4, 6 and 8 gpm/ft^2) are given in Table 6 and Table 7 respectively. Filtration coefficients for 3 different media sizes (0.595 mm, 0.841 mm and 1.19 mm) at a filtration rate of 6 gpm/ft^2 are given in Tables 8 and 9.

Run 17 was made using an increased depth of 30 inches in some of the filters (Filter A was 30 inches deep; Filter B, 30 inches; Filter C, 18 inches; Filter D, 12 inches; Filter E, 18 inches). Filter media diameters were 1.19 mm for Filter A, 0.841 mm for Filters B, C and D and 0.595 mm for Filter E as in previous runs. Filters C and D were operated in series. Filter C which was the first column in series was easily disturbed by variations in the filtration rate and pressure even with the small rate change that occurred during sampling except in the early stages of a run. However, flocs detached during the sampling periods were entrapped completely by Filter D which was the second column in the series. Run 18 was made with the same filters that were used in Run 17 but Filters C and D were operated in parallel. The results of Run 17 and Run 18 are summarized in Table 10.

Table 4. Filtration coefficients for a 10-in filter depth at different filtration rates[a]

Run No.	Influent con. (mg/l)	Filtration rate (gpm/ft^2) 4 K	4 σ_u	6 K	6 σ_u	8 K	8 σ_u
3	4.1	18.68	3.68	16.88	3.88	18.98	4.01
6	6.24	16.67	2.93	17.95	3.18	13.73	4.13
4	7.59	25	3.43	21.3	4.5	19.35	5.32

[a]Media size = 0.841 mm, K in 1/g-hr, σ_u in g/l.

Table 5. Filtration coefficients for a 10-in filter depth with different media sizes[a]

Run No.	Influent conc. (mg/l)	Media diameter (mm) 0.595 K	0.595 σ_u	0.841 K	0.841 σ_u	1.19 K	1.19 σ_u
3	4.1	15.54	4.94	16.88	3.88	34.6	2.61
6	6.24	13.33	4.09	17.95	3.18	16.83	2.96
4	7.59	13.57	7.28	21.3	4.5	35.3	2.90

[a]Filtration rate = 6 gpm/ft^2, K in 1/g-hr, σ_u in g/l.

Table 6. Attachment coefficient for an 18-in filter depth at different filtration rates[a]

Run No.	Influent conc.	Filtration rate (gpm/ft^2)		
	(mg/l)	4	6	8
9	3.95	57.2	48.2	43.9
16	3.67	57.5	33.1	30.5
12	5.68	34.3	33.7	27
15	5.71	23.7	28.5	25.3
10	7.63	32.9	28.2	23.3
14	7.42	31.1	34.0	27.5

[a]Media size = 0.841 mm, unit in l/g-hr.

Table 7. Filter capacity for an 18-in filter depth at different filtration rates[a]

Run No.	Influent conc.	Filtration rate (gpm/ft^2)		
	(mg/l)	4	6	8
9	3.95	1.543	2.06	2.33
16	3.67	1.778	2.54	2.82
12	5.68	1.795	2.35	3.37
15	5.71	1.925	2.04	2.65
10	7.63	2.66	3.83	5.12
14	7.42	3.07	3.77	4.94

[a]Media size = 0.841 mm, unit in g/l.

Table 8. Attachment coefficient for an 18-in filter depth with different media sizes[a]

Run No.	Influent conc.	Media diameter (mm)		
	(mg/l)	0.595	0.841	1.19
9	3.95	29.5	48.2	40.4
16	3.67	29.9	33.1	21.9
12	5.68	28	33.7	15.95
15	5.71	19.02	28.5	23.9
10	7.63	30	28.2	29.1
14	7.42	48.9	34.0	28.8

[a]Filtration rate = 6 gpm/ft^2, unit in 1/g-hr.

Table 9. Filter capacity for an 18-in filter depth with different media sizes[a]

Run No.	Influent conc.	Media diameter (mm)		
	(mg/l)	0.595	0.841	1.19
9	3.95	3.02	2.06	1.712
16	3.67	2.87	2.54	2.43
12	5.68	2.69	2.35	4.27
15	5.71	2.76	2.04	2.32
10	7.63	3.94	3.83	3.43
14	7.42	3.02	3.77	3.68

[a]Filtration rate = 6 gpm/ft^2, unit in g/l.

Table 10. Filtration coefficients for Run 17 and Run 18[a]

Media dia. (mm)	Filter	Filter depth (in)	Run 17		Run 18	
			K	σ_u	K	σ_u
1.19	A	30	19	1.894	19.58	1.686
0.841	D	12	—	—	20.6	2.95
0.841	C	18	—	—	21.3	2.32
0.841	B	30	21.3	1.701	19.48	1.694
0.841	C,D[b]	30	19.18	1.924	—	—
0.595	E	18	23.2	2.34	17.7	2.61

[a]Filtration rate = 6 gpm/ft^2, influent conc. was 5.95 mg/l for Run 17 and 5.74 mg/l for Run 18, K in l/g-hr, σ_u in g/l.

[b]Filters C and D were operated in series.

Calculation of head loss constants

A plot of the head loss data versus the computed total deposit for each filter was not a straight line but a logarithmic plot was reasonably straight. A linear regression on the logarithms of the head loss and deposit data was done and the values for the intercept and the slope were determined. The constants, a and b, for runs with an 18-in filter depth are shown in Table 11 and those for Runs 17 and 18 are in Table 12, where a and b are defined as:

$$\log a = \text{intercept}$$

$$b = \text{slope}$$

and are the filter constants used in Equation 53:

$$H = H_o + a\left[\sigma_u L - \frac{V}{K} \ln \left[\exp (KC_o t) + \exp (K\sigma_u L/V) - 1\right] + C_o V t\right]^b \quad (53)$$

where H and H_o were measured in mm of head loss; σ_u, g/l; K, l/g-hr; V, m/hr; C_o, g/l; and L in m.

Table 11. Head loss constants for 18-in filter runs

Run No.	C_o (mg/l)	d (mm)	V (gpm/ft^2)	a	b	R^2 (%)
9	3.95	0.595	6	1950	1.49	99.4
		0.841	4	933	1.36	98.2
		0.841	6	1148	1.48	99.5
		0.841	8	1202	1.54	99.4
		1.19	6	646	1.47	99.3
16	3.67	0.595	6	1380	1.35	99.8
		0.841	4	661	1.41	98.7
		0.841	6	724	1.35	99.1
		0.841	8	776	1.28	98.6
		1.19	6	490	1.44	99.6
12	5.68	0.595	6	3020	1.38	99.8
		0.841	4	1230	1.25	99.9
		0.841	6	1413	1.23	99.5
		0.841	8	1549	1.33	99.9
		1.19	6	646	1.23	99.6
15	5.71	0.595	6	2340	1.35	99.8
		0.841	4	912	1.25	99.8
		0.841	6	1230	1.27	99.8
		0.841	8	1318	1.30	100
		1.19	6	631	1.32	99.7
10	7.63	0.595	6	2880	1.37	99.6
		0.841	4	1445	1.26	99.8
		0.841	6	1738	1.37	99.9
		0.841	8	1622	1.39	99.8
		1.19	6	724	1.24	99.7
14	7.42	0.595	6	3467	1.45	99.1
		0.841	4	1445	1.33	99.8
		0.841	6	1660	1.38	99.8
		0.841	8	1585	1.35	99.6
		1.19	6	741	1.26	99.6

Table 12. Head loss constants of Run 17 and Run 18[a]

Run No.	C_o (mg/l)	Filter	D (mm)	L (in)	a	b	R^2 (%)
17	5.95	A	1.19	30	676	1.27	99.4
		B	0.841	30	1318	1.39	99.9
		C,D[b]	0.841	30	977	1.13	99.9
		E	0.595	18	2400	1.33	99.8
18	5.74	A	1.19	30	646	1.18	99.6
		B	0.841	30	1349	1.24	99.8
		C	0.841	18	1230	1.29	99.9
		D	0.841	12	1259	1.32	100
		E	0.595	18	2570	1.33	99.9

[a]Filtration rate = 6 gpm/ft^2.

[b]Filters C and D were operated in series.

RESULTS AND DISCUSSION

Effects of Filtration Rate, Influent Concentration and Media Size on Filtration Coefficients and Head Loss Constants

The breakthrough curve is a plot of C/C_o versus time, t. This curve is S-shaped and is described by Equation 46. The full curve increases exponentially at first and then levels off as C/C_o approaches 1. Since the starting C/C_o value for a short filter is relatively high, the curve follows only the latter part of the S-shaped curve and the C/C_o increase during the filter run is usually small. Therefore, small changes in the breakthrough curve resulting from run-to-run variations and random behavior of the filter could cause large variations in the filtration coefficients. This may be the reason why the filtration coefficients for 10-in filters are so difficult to analyze, especially for the effects of influent concentration. Data, mostly from the 18-in and 30-in filters, will be used to relate the filtration coefficients and head loss constants to the physical parameters.

As was mentioned in the literature review section, a number of physical and chemical parameters will affect the performance of a deep bed filter. The pH of the suspension will affect the surface charge of the iron floc. Above the

pH of the zero point of charge, iron flocs are negatively charged and below that they are positively charged. All filter runs were made near a pH of 8.5 which was reported to be the zero point of charge for amorphous ferric hydroxide (52). So the electrical double layer repulsion was probably insignificant compared to other forces. Therefore, only the van der Waals' attractive forces should predominate for the attachment of particles on the filter grain surface at the pH that existed during the filter runs.

Particle sizes and zeta potentials were not measured in this study, but some information on iron hydroxide floc can be found in the results of previous investigators. Cleasby (7) observed that precipitated iron under aerated conditions had particle sizes ranging from 1-20 microns with a majority of the particles being about 5 microns in size. Heertjes and Lerk (13,14) found that the particle size of a well-flocculated ferric hydroxide suspension usually varied between 0.1 and 10 microns, that the electrokinetic charge was negligible and that the density of the iron hydroxide flocs was about 1.004 g/cm^3.

The kinetic equation of Iwasaki's filtration model is Equation 6:

$$\frac{\partial \sigma}{\partial t} = \lambda V C$$

The kinetic equation for this study is:

$$\frac{\partial \sigma}{\partial t} = K(\sigma_u - \sigma)C$$

At $t = 0$, $\lambda = \lambda_o$ and $\sigma = 0$:

$$\lambda_o VC = K\sigma_u C$$

or

$$\lambda_o = \frac{K\sigma_u}{V} \tag{59}$$

Many attempts have been made to find a relationship between the filtration rate and the initial filter coefficient. From Equation 59 the author's results can be compared to the investigations of others.

Regression analyses were done to fit the filtration coefficients obtained from runs using the 18-in filter depth to filtration rate, influent concentration and media size using MINITAB, a computer program for statistical analysis. Using all of the data

$$K = 147.9C_o^{-0.319}{}_D{}^{-0.215}{}_V{}^{-0.396} \tag{60}$$

$(R^2 = 21.3\ \%)$

$$\sigma_u = 0.1285 C_o^{0.668} D^{-0.0928} V^{0.719} \quad (61)$$
$$(R^2 = 65.1\ \%)$$

where K in l/g-hr, σ_u in g/l, C_o in mg/l, D in mm, V in m/hr.

Using the data from the filters with a grain size of 0.841 mm:

$$K = 240 C_o^{-0.605} V^{-0.363} \quad (62)$$
$$(R^2 = 56\ \%)$$

$$\sigma_u = 0.1094 C_o^{0.777} V^{0.705} \quad (63)$$
$$(R^2 = 77.6\ \%)$$

From the data at a filtration rate of 6 gpm/ft^2:

$$K = 30.9 C_o^{-0.048} D^{-0.215} \quad (64)$$
$$(R^2 = 5.1\ \%)$$

$$\sigma_u = 1.085 C_o^{0.557} D^{-0.0928} \quad (65)$$
$$(R^2 = 39.7\ \%)$$

The effects of filtration rate on the filtration coefficients are shown in Figures 14 and 15. The effects of

media size are shown in Figures 16 and 17. And, the effects of influent concentration are shown in Figures 18 and 19. The figures show that the effects of these variables are quite different from run to run. Unaccountable factors affect run-to-run variations. Even during a run, they affect filter-to-filter variations. Unaccountable factors for run-to-run variations could be chemical changes such as pH, ionic strength and ionic species in suspension or different initial surface characteristics of media caused by particle deposits remaining after backwash. There will also be filter-to-filter variations even when the filters are essentially the same in construction and in the way they are being operated.

Additional results from regression analyses are given in the Appendix to demonstrate these run-to-run and filter-to-filter variations. Equations 60-65 include not only the effects of the tested variables, but also run-to-run and filter-to-filter variations. The first two parts of the Appendix demonstrate that regression can explain more by elimination of run-to-run variations. However, unaccountable factors still affect the performance of filters even in parallel operations using the same influent. From the regression results, it may be said that the filter capacity, σ_u, is less affected than the attachment coefficient, K, by these unaccountable factors.

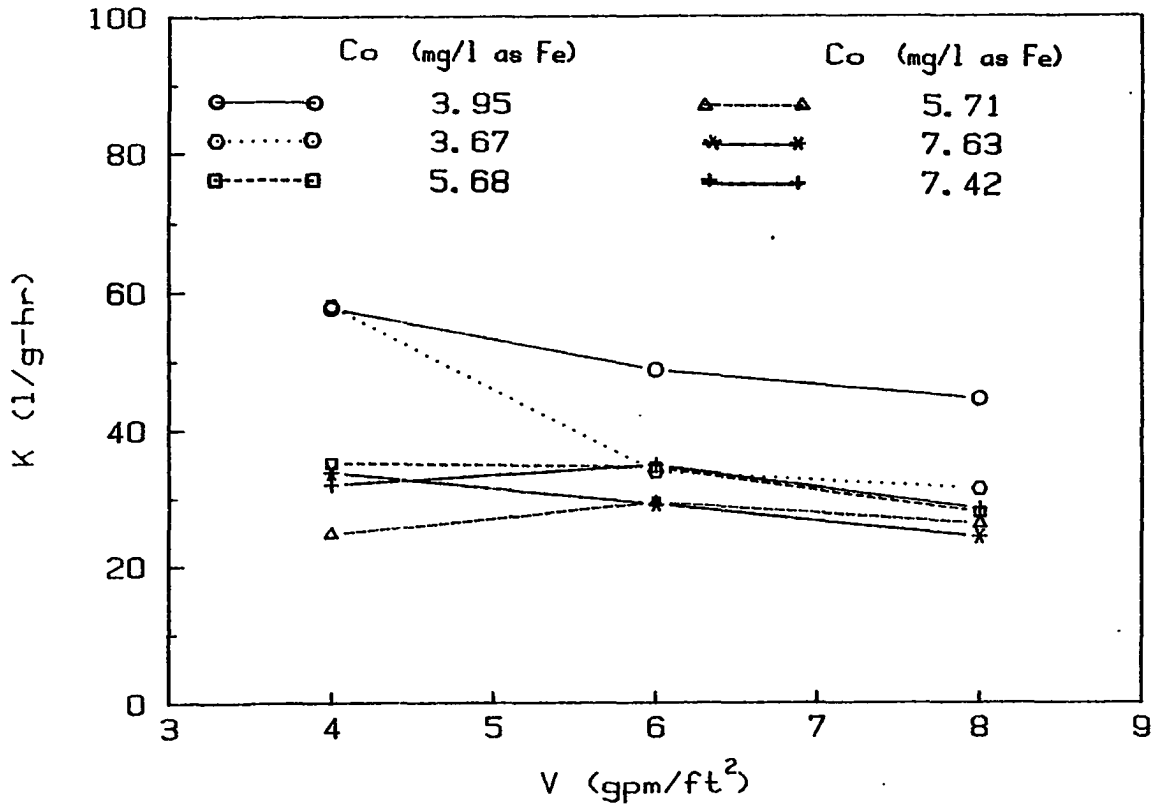

Figure 14. Effect of filtration rate on K for 18-in filters with 0.841 mm media

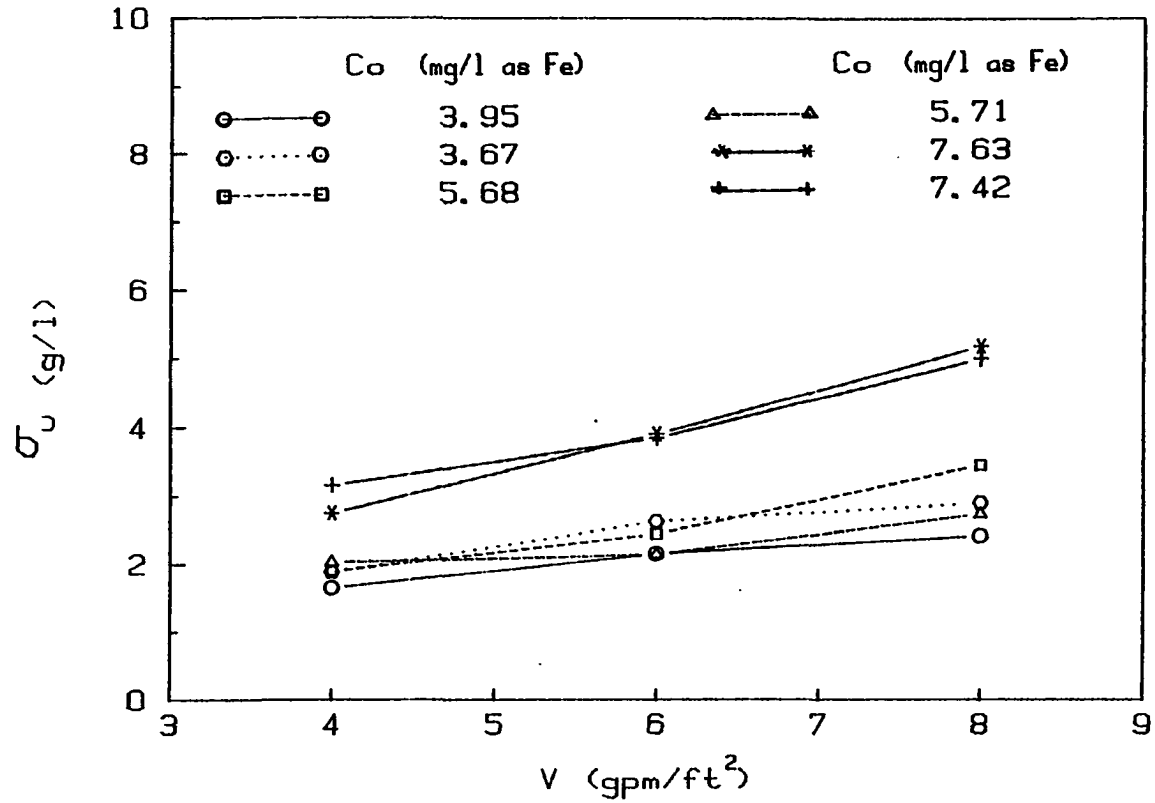

Figure 15. Effect of filtration rate on σ_u for 18-in filters with 0.841 mm media

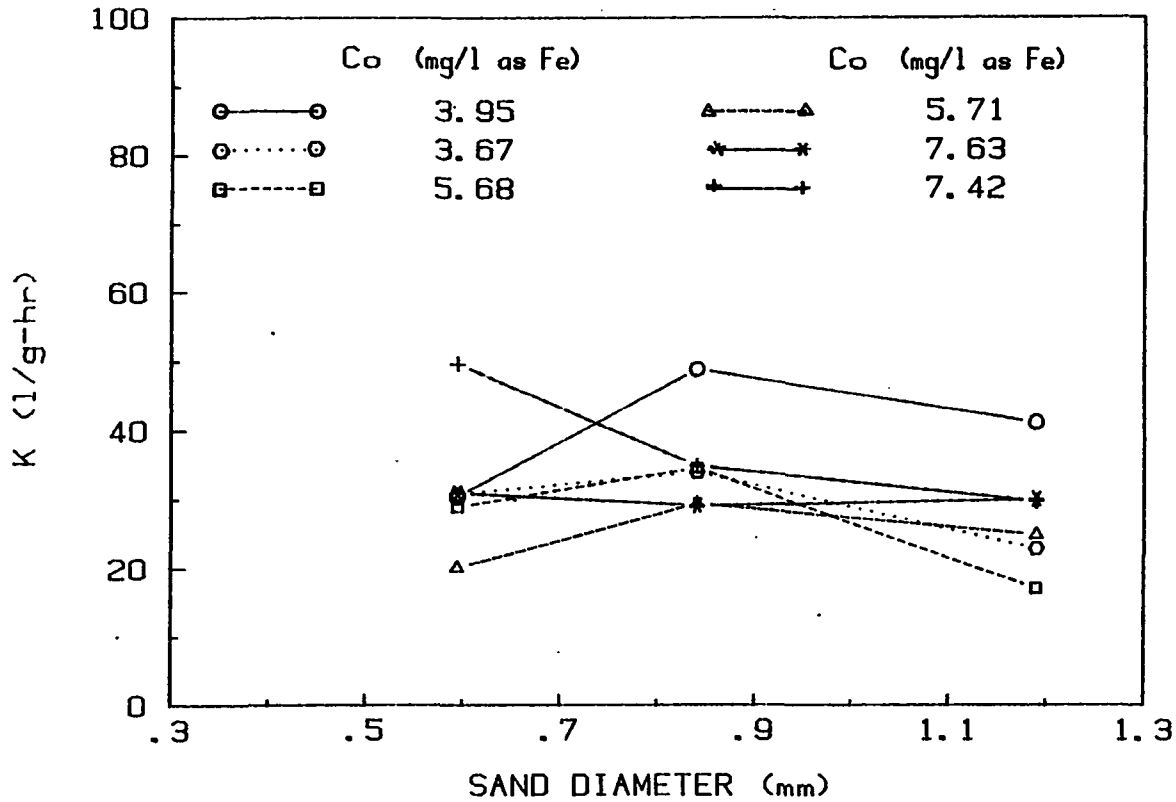

Figure 16. Effect of media size on K for 18-in filters at a filtration rate 6 gpm/ft^2

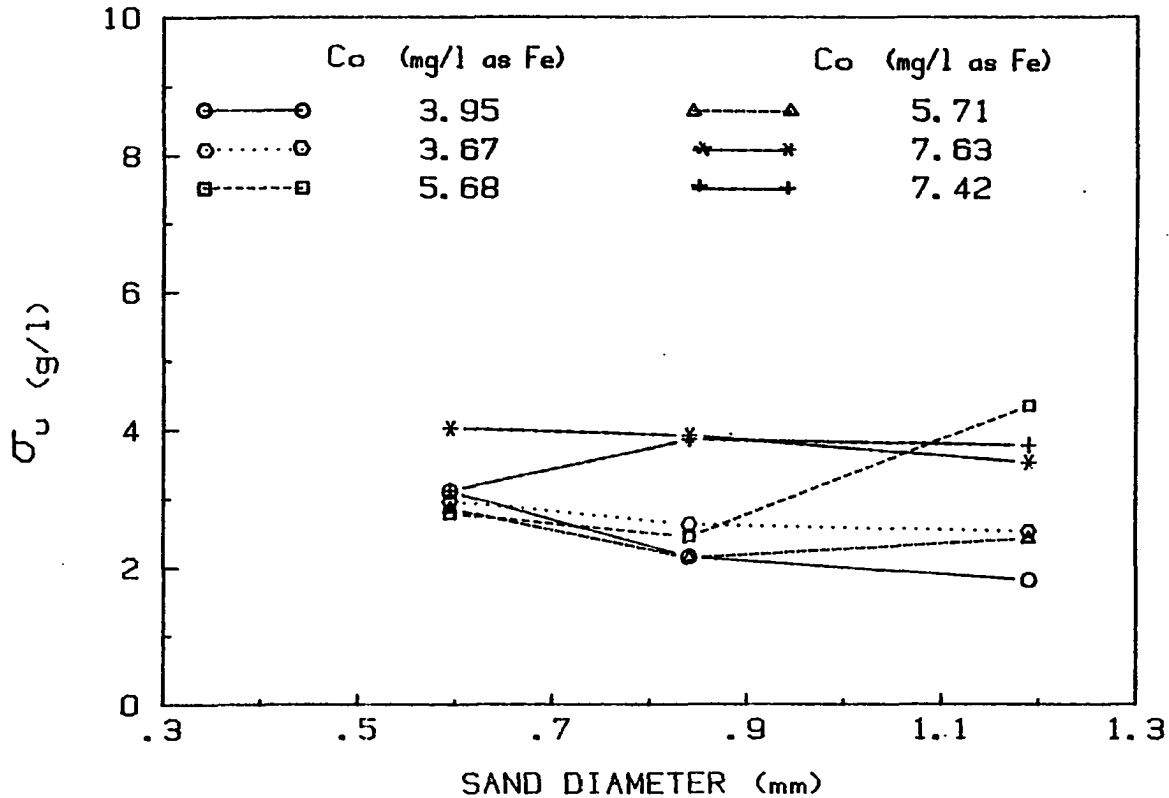

Figure 17. Effect of media size on σ_u for 18-in filters at a filtration rate 6 gpm/ft^2

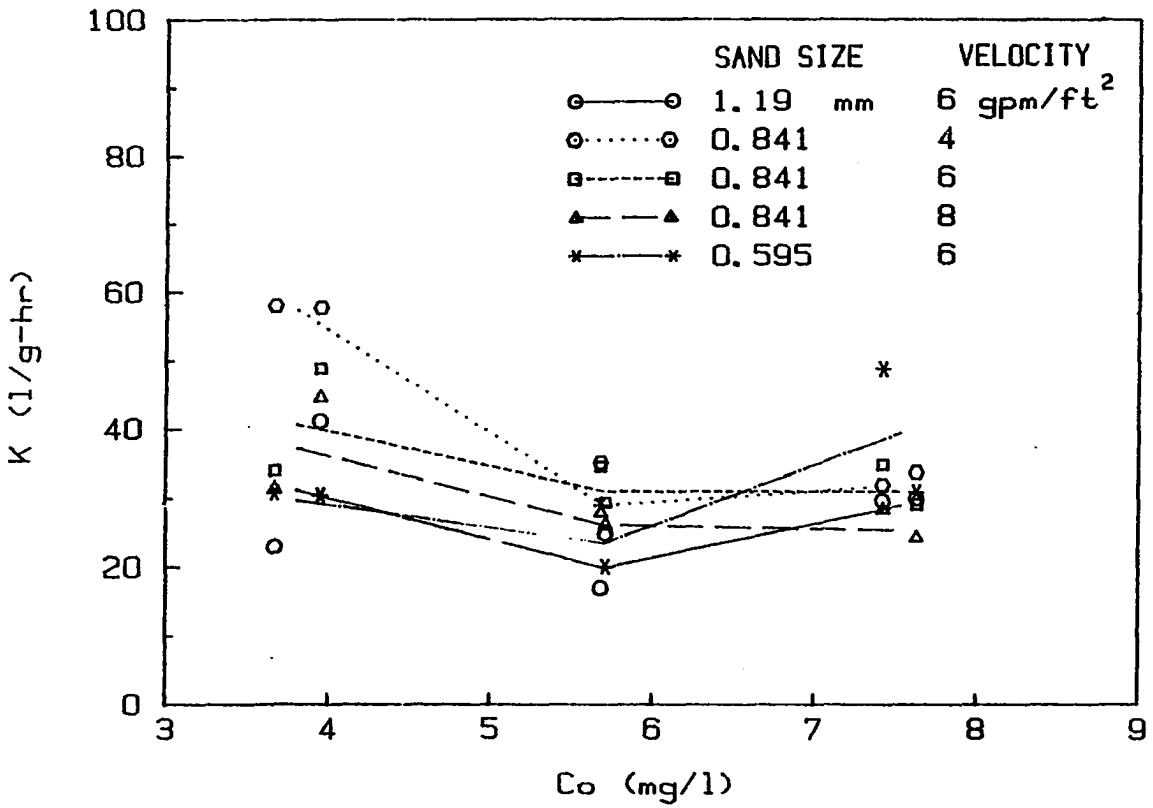

Figure 18. Effect of influent concentration on K for 18-in filters

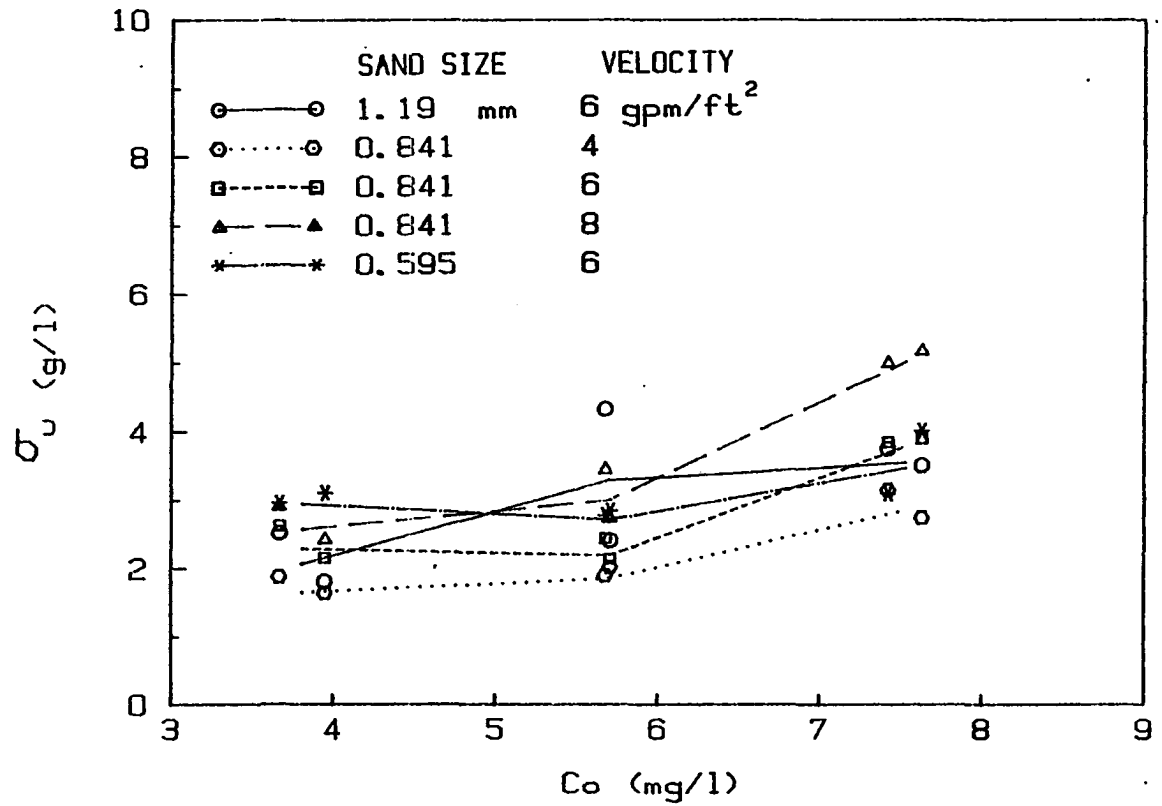

Figure 19. Effect of influent concentration on σ_u for 18-in filters

From the Appendix, the relationships between the filtration coefficients and the filtration rates are in the range of:

$$K \propto V^{-0.118} \text{ to } V^{-0.944} \tag{66}$$

$$\sigma_u \propto V^{0.440} \text{ to } V^{0.942} \tag{67}$$

with high R^2. Increasing the filtration rate will increase the filter capacity since it increases the penetration of particles deeply into the filter bed but the attachment coefficient will decrease.

In the derivation of Equation 45, the attachment coefficient, K, was expected to be a function of the filtration rate and the space available for particle deposition, $\sigma_u - \sigma$. From the experimental results, K appears to be a function of the filtration rate as was expected. The fact that plots of $-\ln (C_o/C - 1)$ versus t were fairly linear for the most of the filter runs does not necessarily indicate that K is not dependent on $\sigma_u - \sigma$. But, during the part of the filtration cycle used in the calculations, the effect of deposit on K appears to be insignificant. The density of deposits may increase by compaction effects as filtration proceeds. It may reduce the effect of $\sigma_u - \sigma$ on the attachment coefficient.

According to Equation 59 by using the simple averages for the coefficients in Equation 66 and 67

$$\lambda_o \propto V^{-0.531_V 0.691_V - 1}$$

or

$$\lambda_o \propto V^{-0.84} \tag{68}$$

According to the observations by Cleasby (7), and Heertjes and Lerk (13,14), iron flocs should be bigger than 1 micron and therefore diffusive deposition should not be important. Only London-van der Waals attractive forces and gravity force should be important in these filter runs. From Rajagopalan and Tien's Equation 34, λ_o is approximately equal to the London-van der Waals forces term + the gravity term or:

$$\lambda_o = pV^{-1/8} + qV^{-1.2}$$

where p and q are constants.

The exponent of Equation 68 lies between -1/8 and -1.2 and seems to be in agreement with the prediction by their model. Even if the extremes in the coefficients from Equation 66 and 67 are combined, the range given by Rajagopalan and Tien are reasonably well mapped. That is, λ_o is proportional to

$V^{-0.176}$ to $V^{-1.504}$.

The dependence of the filtration coefficients on media size is in the range (from the Appendix):

$$K \propto D^{-0.813} \text{ to } D^{0.453} \tag{69}$$

$$\sigma_u \propto D^{-0.819} \text{ to } D^{0.667} \tag{70}$$

The exponents of both equations varied widely and had a relatively low R^2 value. The slopes of the curves in Figures 16 and 17 are nearly horizontal and it may be said that media size has little effect on the filtration coefficients.

The effects of influent concentration on the filtration coefficients were in the range of:

$$K \propto C_o^{-0.914} \text{ to } C_o^{-0.367} \tag{71}$$

(neglecting regressions with low R^2)

$$\sigma_u \propto C_o^{0.663} \text{ to } C_o^{0.925} \tag{72}$$

According to Equations 71 and 72, increasing the influent concentration increases the filter capacity, but decreases the attachment coefficient. Particles may have more chance to penetrate deeper into the filter bed at the high particle flux associated with a high influent concentration, resulting

in a high filter capacity. A high particle flux will result in a large volume of deposit, constricting the flow paths. Therefore, a high influent concentration may bring about a low attachment coefficient. The particle size may vary with varying influent concentration since there may be more chances for flocculation at a high concentration. In this study, particle sizes were not measured and no information is available as to whether the particle size varies with influent concentration or not.

Regression analyses to fit the head loss data to the calculated total particle deposits yielded very high R^2 values and this implies that the relation between head loss and total deposit in the filter can be represented by Equation 53. The magnitude of the head loss is mainly affected by the value of constant a. The value of constant b indicates the rate at which the head loss will increase as clogging proceeds. The constant a from runs using an 18-in filter depth was related to the variables tested as follows:

$$a = 2.57 \times 10^4 C_o^{0.806} D^{-1.9} V^{0.306} \qquad (73)$$

$$(R^2 = 92.8\ \%)$$

where C_o in g/l, D in mm and V in m/hr.

and the constant b from runs using an 18-in filter depth

by:

$$b = 0.719C_o^{-0.0864}{}_D{}^{-0.0785}{}_V{}^{0.0614} \qquad (74)$$

$$(R^2 = 28.9\ \%)$$

The regression analysis explains the effects of the variables on constant a very well, but only 28.9 % of the variation of b is explained. The rest of the variation could be due to random variations in the filter performance and run-to-run variations. However, the constant b is in the range of 1.23 to 1.54 and it does not have a large range in values as the constant a.

The distribution of deposit in the filter bed may affect the head loss development as has been demonstrated by Letterman (30). For example, a uniform distribution of deposits with respect to depth in the filter will develop less head loss than a skewed distribution does. In the operation of Filters C and D in series at Run 17, the first filter would frequently shed floc when disturbed but the detached flocs were entrapped in the second filter. Therefore, deposits were more evenly distributed than those in a single column filter, resulting in low head loss with low values for constants a and b.

Sensitivity analysis of Filtration Coefficients on Filter Performance

By making changes in the filtration coefficients, one-by-one in Equation 46, it was possible to observe the changes in the breakthrough curve, and therefore to assess the sensitivity of filter performance to the filtration coefficients. Thus, a sensitivity analysis provided a basis for determining how much the attachment coefficient, K, and the filter capacity, σ_u, can vary and still predict the breakthrough curve fairly well.

A plot of $-\ln (C_o/C - 1)$ versus t gives a straight line with a slope of KC_o and an intercept $-\ln [\exp (K x \sigma_u/V) - 1]$. The intercept on the t axis, t_{50}, represents the time at which the effluent concentration, C, becomes half as great as the influent concentration, C_o, and is the time at which 50 % of filter capacity is assumed to be exhausted:

$$t_{50} = \ln [\exp (K x \sigma_u/V) - 1]/(KC_o) \qquad (75)$$

The values of K and σ_u can be modified by changing the filtration rate, influent concentration, media size, chemical dosage of filter aids, etc. Increasing σ_u results in a shift of the $-\ln (C_o/C - 1)$ versus t line to the right

by increasing the intercept value on the time axis, t_{50}, but it does not change the slope of the line. Therefore, increasing σ_u has the effect of delaying the beginning of effluent degradation stage because it makes the intercept on the $-\ln (C_o/C - 1)$ axis more negative. Increasing K makes the slope steeper and changed the intercept on the time axis, t_{50}. For $\exp (Kx\sigma_u/V) >> 1$, t_{50} becomes:

$$t_{50} \approx \frac{\sigma_u x}{C_o V}$$

The position of t_{50} does not change very much with variations in K. As a result, increasing K makes the breakthrough curve rise more abruptly, but t_{50} remains almost the same.

Figures 20 and 21 illustrate the effect of varying K on the $-\ln (C_o/C - 1)$ versus t line and on the breakthrough curve. The effect of varying σ_u is shown in Figures 22 and 23. Based on Figures 21 and 23 the breakthrough curve appears to be more sensitive to the variation in σ_u than those in K. Therefore, a small variation in filter performance can result in large variation of K but much smaller variations in σ_u. This may be one of the reasons why so much of the variation in K was not explained by regression analysis. The reason for the differences in sensitivity to K and σ_u may be inherent in the nature of K and σ_u. The filter capacity, σ_u

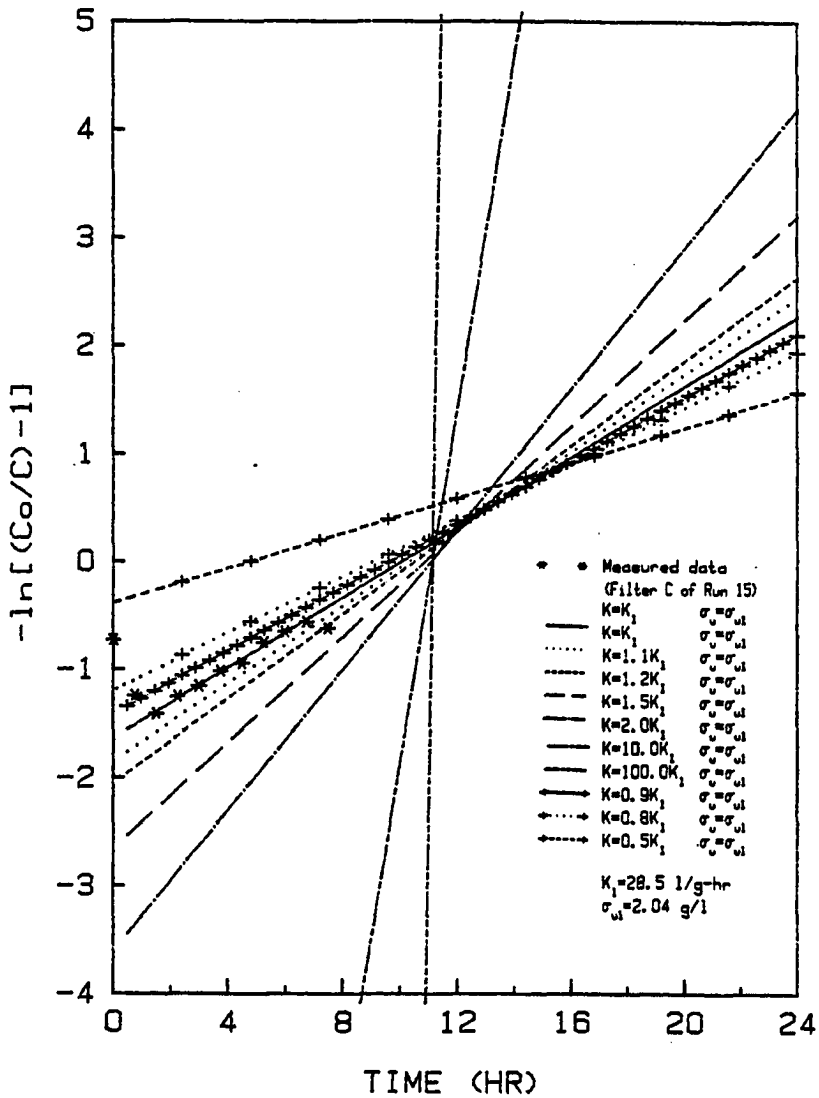

Figure 20. Effect of K on $-\ln (C_o/C - 1)$ versus t curve

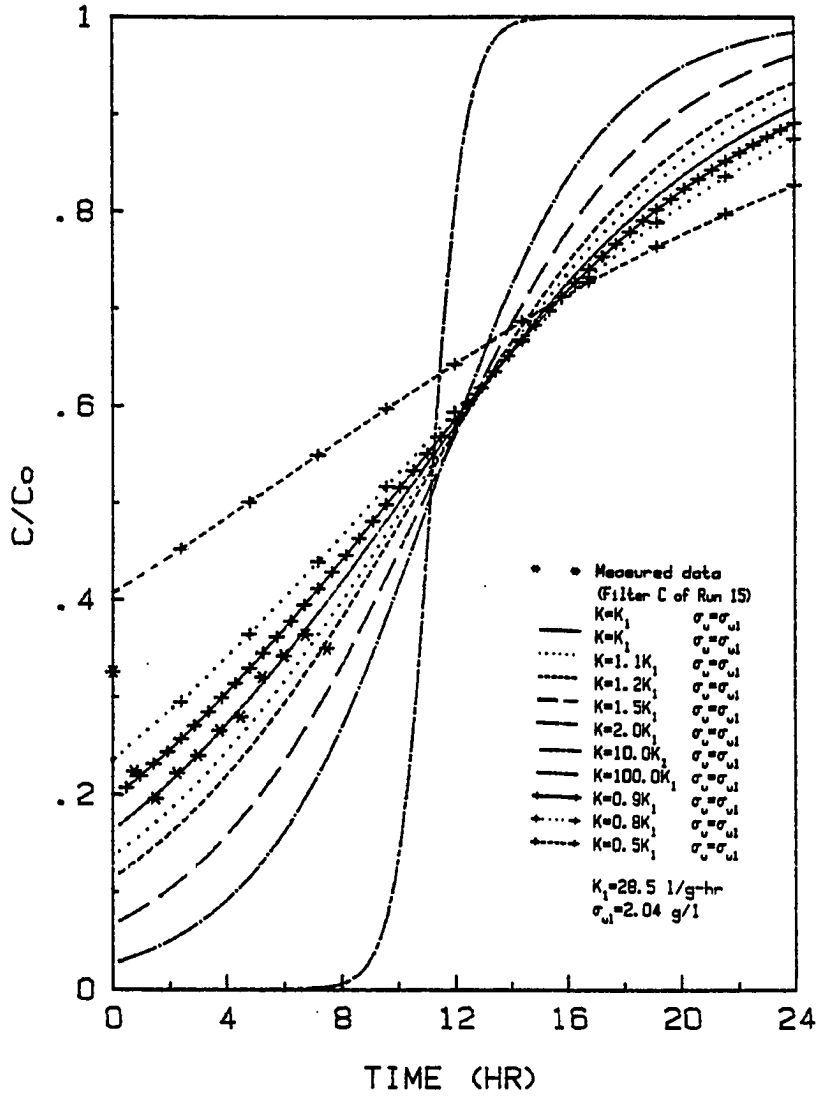

Figure 21. Effect of K on the breakthrough curve

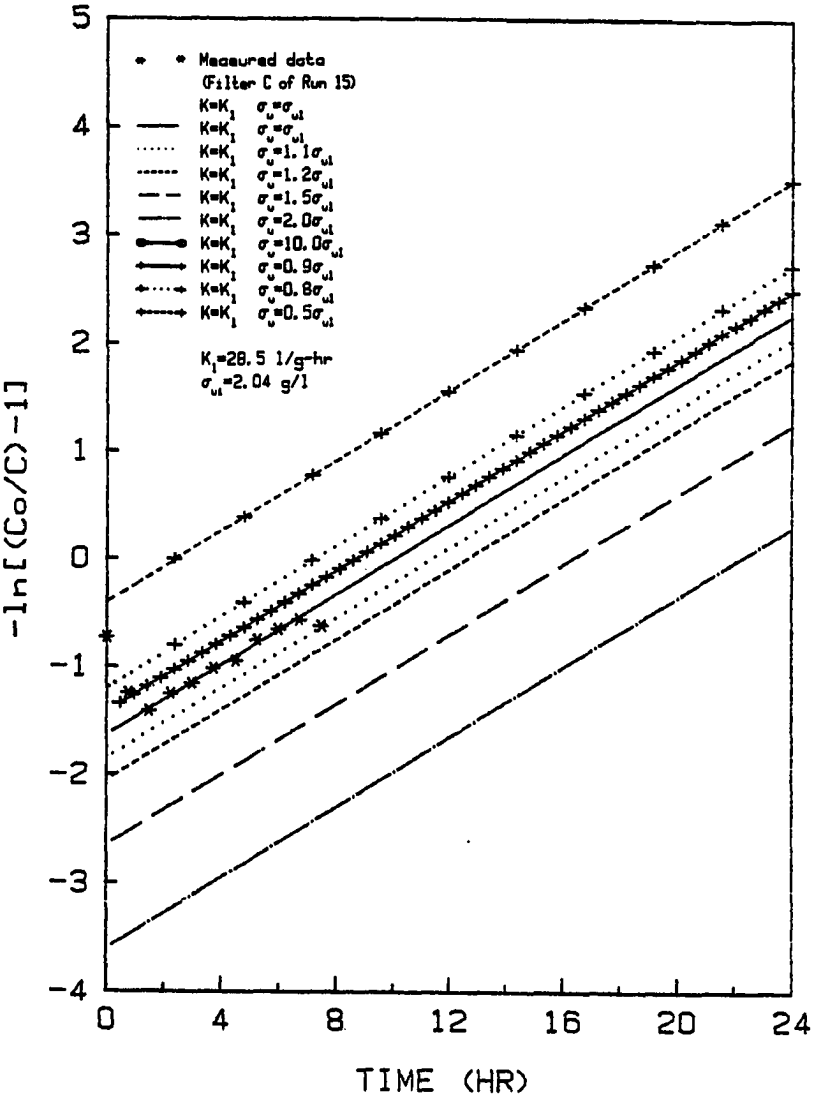

Figure 22. Effect of σ_u on $-\ln (C_o/C - 1)$ versus t curve

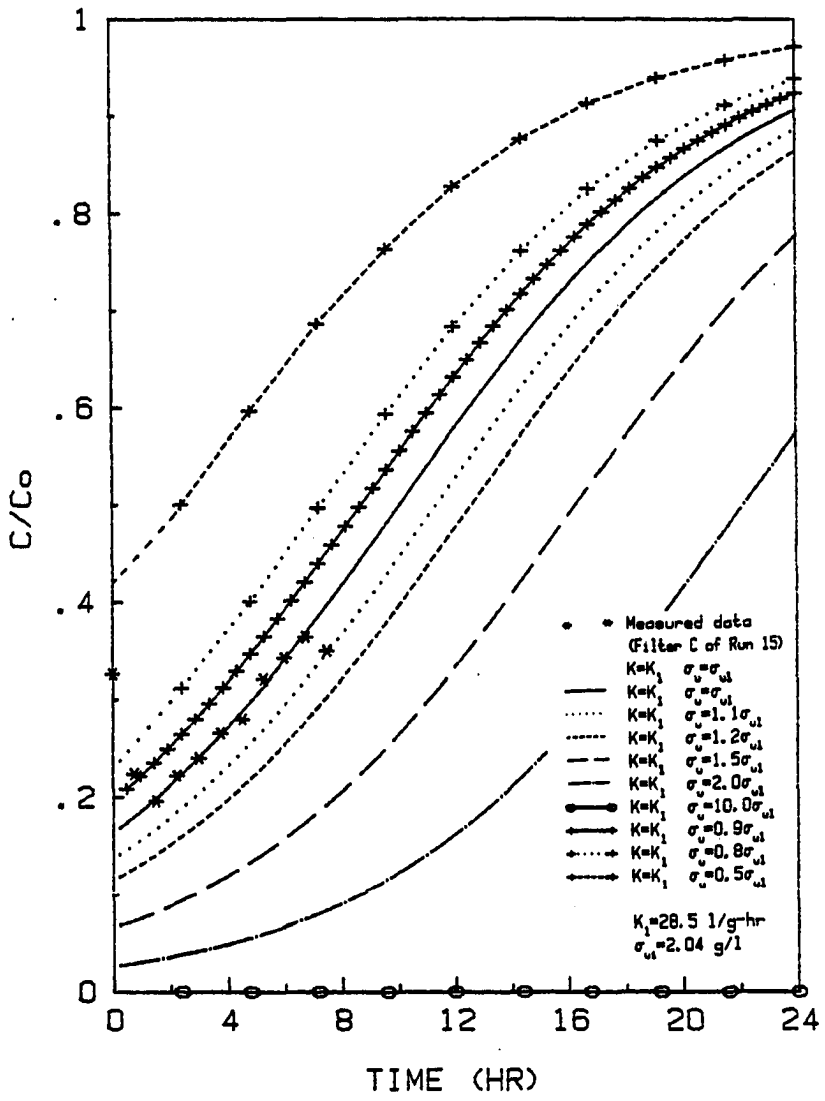

Figure 23. Effect of σ_u on the breakthrough curve

represents the maximum quantity of deposit which a filter can hold in a unit volume of filter and the attachment coefficient, K represents the retention probability of particles while they pass through a unit volume of filter. The ultimate deposit probably reaches about the same value no matter how the filtration progress has been affected by random variations in the suspension and deposition in the filter. But, K will be sensitive to these variations.

Effect of Filter Depth on Filter Performance

Three different filter depths 10, 18, 30 inches were used throughout the filter runs to determine the effects of filter depth on performance. Increasing the filter depth decreased the filter capacity, σ_u, but did not have a consistent effect on the attachment coefficient, K. As shown earlier, σ_u was explained more by the regression analysis than K. In other words, K had more unexplained variation than σ_u. The depth effect on K may also behave this way. In Run 18, the effect of depth on the filtration coefficients was clearly demonstrated. Where results from a number of runs were pooled, the effects were not so clearly demonstrated because of uncontrollable differences in the way that the filters were operated from run to run.

The filtration equations that have been derived

presuppose a media with a uniform size. Filter sand prepared by sieving can not be absolutely uniform in size and should therefore be represented by a size distribution. The backwashing process will stratify the finest sand at the top of the filter and the coarsest at the bottom. Clogging of top layers will be intensified, and the top layers will be utilized more effectively than the bottom layers. Since the filter capacity is expressed as a weight of particles deposited in a unit volume of filter, the shorter the filter depth, the more fully will the filter capacity be utilized. This presupposes, of course, a run of sufficient length so that some clogging in the upper layers of the filter can occur.

As was discussed in an earlier chapter on model development, the head loss through a filter should be proportional to some power of total deposit that is in it. A great part of the particles deposited in the filter are in the top layer since usually only the top layers are intensively clogged. Therefore, it is likely that the same portions of the filter are responsible for head loss development for filters of different depths. This may be the reason why varying the filter depth appeared to have so little effect on the head loss constants a and b as is illustrated in Tables 11 and 12.

An important question to be answered is whether

information obtained from the testing of pilot filters with a shallow depth of media can be used for the design of a full depth filter. A higher filter capacity should be obtained for a shorter filter than for a longer filter. Since a higher filter capacity delays the beginning of degradation stage, use of a filter capacity derived for a short filter for the design of a long filter should result in breakthrough occurring at an earlier time than that predicted. The head loss constants, a and b, may be used in the filter design without any such problem since they do not seem to be affected by variations in depth. As a consequence of the depth and concentration effects, it is apparent that pilot plant tests employing several depths of media and encompassing a range of influent concentration are needed to obtain the filtration coefficients needed for design. The filter capacity of the water tested in this study was a function of both depth and concentration. The attachment coefficient appeared to be a function of other variables, probably the chemical and physical properties of the suspension itself.

CONCLUSIONS

A kinetic equation based on filtration mechanisms was obtained that is identical to the limited growth model. The analytical solution of the kinetic equation and material balance equation successfully describes the breakthrough curves for filtration. The solids retention characteristics of a filter is described by the filter capacity, σ_u, and the attachment coefficient, K.

These parameters can be obtained by a regression analysis on data obtained from pilot plant operation. In the filtration of an iron hydroxide suspension, the filter capacity, σ_u, increased as either the filtration rate, V, or the influent concentration, C_o, increased. The attachment coefficient, K, increased as either the filtration rate, V, or the influent concentration decreased. The media size seemed to have little effect on the filtration coefficients.

From a sensitivity analysis performed on the filtration coefficients, it was found that the beginning of effluent degradation stage is delayed as the filter capacity, σ_u, increases. The breakthrough curve rises abruptly as K increases but the time when the effluent concentration

reaches one half of the concentration of the influent concentration remains almost the same throughout the practical range in values for K for a given value of σ_u.

Head loss through the filter depth was expressed as a power of the total particle deposit in the filter. Equation 47 was used to calculate the total deposits. The constant, a, increased as the filtration rate increased, as the influent concentration increased and as the media size decreased. The constant, b, did not change very much, and probably was dependent on random variations related to the chemical and physical properties of the suspension. Varying the depth appeared to have little effect on the head loss constants, but the filter capacity decreased as the filter depth increased. Depth seemed to have little effect on the attachment coefficient.

The media size that is selected will affect the performance by limiting the quality of effluent that can be produced by a given filter. A finer grained media will produce greater clarity than a coarser grained media. Therefore, the media size sets a lower limit on the clarity that can be obtained with a filter. This cannot, in fact, be predicted by the breakthrough curve equation. The effect of media size is to cause a break to occur in the plot of $-\ln (C_o/C - 1)$ versus t so that even without the initial ripening period, there would be limits placed on the initial

effluent quality that are related to media size. Further study will be needed to make these effects predictable. However, it can be reported that media size does not seem to affect the numerical value of either of the filtration coefficients. The effects of media size appear to be related to determining the limiting clarity that can be achieved by the filter and the head loss that will be spent during the filter run.

The breakthrough curve equation and the head loss equation provide a serviceable method for mathematically describing the performance of a filter. Based on these equations and derived values for filtration coefficients and head loss constants, it should be possible to determine the optimum choice of depth and media size in the design of a deep bed filter. However, this study indicates that the pilot plant tests used in determining the filtration coefficients and head loss constants cannot be limited to a single depth of filter and a single influent concentration unless that depth and concentration happens to be the same as the values expected in the completed system.

BIBLIOGRAPHY

1. Adin, A. Solution of granular bed filtration equations. J. Env. Eng. Div., Proc. ASCE, 104 (EE3), (1978), 471-484.

2. Adin, A., and Rebhun, M. A model to predict concentration and head loss profiles in filtration. J. AWWA, 69 (8), (1977), 444-453.

3. Amirtharajah, A., and Wetstein, D. P. Initial degradation of effluent quality during filtration. J. AWWA, 72 (9), (1980), 518-524.

4. Benefield, L. D., Judkins, J, F., and Weand, B. L. Process Chemistry for Water and Wastewater Treatment. Englewood Cliffs: Prentice-Hall Inc., 1982.

5. Bohart, G. S., and Adams, E. Q. Some aspects of the behavior of charcoal with respect to chlorine. J. American Chemical Society, 42, (1920), 523-543.

6. Camp, T. R. Theory of water filtration. J. San. Eng. Div., Proc. ASCE, 90 (SA4), (1964), 1-30.

7. Cleasby, J. L. Selection of optimum filtration rates for sand filters. Unpublished Ph.D. thesis, Iowa State University, Ames, Iowa, 1960.

8. Cleasby, J. L., and Baumann, E. R. Selection of sand filtration rates. J. AWWA, 54,(1962), 579-602.

9. Deb, A. K. Theory of sand filtration. J. San. Eng. Div., Proc. ASCE, 95 (SA3), (1969), 399-422.

10. Fitzpatrick, J. A., and Spielman, L. A. Filtration of aqueous latex suspensions through beds of glass spheres. J. Colloid Interface Sci., 43 (2), (1973), 350-369.

11. Ghosh, M. M., Jordan, T. A., and Porter, R. L. Physicochemical approach to water and wastewater filtration. J. Env. Eng. Div., Proc. ASCE, 101 (EE1), (1975), 71-86.

12. Hall, W.A. An analysis of sand filtration. J. San. Eng. Div., Proc. ASCE, 83 (SA3), (1957), 1276-1-9.

13. Heertjes, P. M., and Lerk, C. F. The functioning of deep-bed filters. Part I: The filtration of colloidal solutions. Trans. Inst. Chem. Engrs., 45, (1967), T129-T137.

14. Heertjes, P. M., and Lerk, C. F. The functioning of deep-bed filters. Part II: The filtration of flocculated suspensions. Trans. Inst. Chem. Engrs., 45, (1967), T138-T145.

15. Herzig, J. P., Leclerc, D. M., and Le Goff, P. Flow of suspensions through porous media-application to deep bed filtration. Ind. and Eng. Chem., 62 (5), (1970), 8-35.

16. Hutchins, R. A. New method simplifies design of activated carbon systems. Chem. Engr., 80, (1973), 133-138.

17. Ison, C. R., and Ives, K. J. Removal mechanisms in deep bed filtration. Chem. Eng. Sci., 24, (1969), 717-729.

18. Ives, K. J. Rational design of filters. Proc. Inst. Civil Engrs., 16 (1960), 189-193.

19. Ives, K. J. Simplified rational analysis of filter behaviour. Proc. Inst. Civil Engrs., 25, (1963), 345-364.

20. Ives, K. J. Theory of filtration. Special Subject No. 7 in International Water Supply Association Eighth Congress, Vienna, 1969, pp. K1-28.

21. Ives, K. J. The significance of theory. J. Inst. Water Engrs., 25, (1971), 13-20.

22. Ives, K. J. Capture mechanisms in filtration. In The Scientific Basis of Filtration. Ed. K. J. Ives. Netherlands: Noordhoff International Publishers, 1975, pp. 183-201.

23. Ives, K. J. and Gregory, A. Basic concepts in filtration. Proc. Soc. Water Treat. Exam., 16, (1967), 147-169.

24. Ives, K.J., and Pienvichitr, V. Kinetics of the filtration of dilute suspensions. Chem. Eng. Sci., 20, (1965), 965-973.

25. Ives, K. J., and Sholji, I. Research on variables

affecting filtration. J. San. Eng. Div., Proc. ASCE, 91 (SA4), (1965), 1-18.

26. Iwasaki, T. Some notes on sand filtration. J. AWWA, 29 (10), (1937), 1591-1602.

27. Jackson, G. E. Granular media filtration in water and wastewater treatment. Part 1. CRC Crit. Rev. Environ. Control, 11 (10), (1980), 339-373.

28. Jackson, G. E. Granular media filtration in water and wastewater treatment. Part 2. CRC Crit. Rev. Environ. Control, 11 (11), (1980), 1-36.

29. Jobin, R., and Ghosh, M. M. Effect of buffer intensity and organic matter on the oxygenation of ferrous iron. J. AWWA, 64, (1972), 590-595.

30. Letterman, R. D. Optimizing deep bed water filters using a deposit distribution concept. Filtration & Separation, 13, (1976), 343-350.

31. Mackrle, V., and Mackrle, S. Adhesion in filters. J. San. Eng. Div., Proc. ASCE, 87 (SA5), (1961), 17-32.

32. Maroudas, A., and Eisenklam, P. Clarification of suspensions: A study of particle deposition in granular media. Part 2—A theory of clarification. Chem. Eng. Sci., 20, (1965), 875-888.

33. Mints, D. M. Modern theory of filtration. Special Subject No. 10 in Internationnal Water Supply Association Seventh Congress, Barcelona, 1966, pp. P1-29.

34. Mints, D. M., and Krishtul, V. P. Investigation of the process of filtration of a suspension in a granular bed. J. Appl. Chem. of the USSR (English transl.), 33 (2), (1960), 303-314

35. Mints, D. M., Paskutskaya, L. N., and Chernova, Z. V. Mechanism of the filtration process in high-speed water filters. J. Appl. Chem. of the USSR (English transl.), 40 (8), (1967), 1634-1639.

36. O'Melia, C. R., and Stumm, W. Theory of filtration. J. AWWA, 59 (11), (1967), 1393-1412.

37. Oulman, C. .Iron and manganese removal: Problems. Presented at the 20th Annual ASCE Water Resources Design

Conference, Iowa State University, Ames, Iowa, 1982.

38. Oulman, C. S., and Yu, M. J. Effect of specific deposit-hydraulic conductivity relationship on the mathematical analysis of the BDST filtration equation. Unpublished paper, Dept. Civil Engineering, Iowa State University, Ames, Iowa, 1981.

39. Pendse, H., Tien, C., Rajagopalan, R., and Turian, R. M. Dispersion measurement in clogged filter beds: A diagnostic study on the morphology of particle deposits. J. AIChE, 24 (3), (1978), 473-485.

40. Rajagopalan, R. The theory of deep bed filtration. In Progress in Filtration and Separation. Ed. R. J. Wakeman. New York: Elsevier, 1979, pp. 179-269.

41. Rajagopalan, R. and Tien, C. Single collector analysis of collection mechanisms in water filtration. Can. J. Chem. Eng., 55, (1977), 246-255.

42. Saatci, A. M. Application of adsorption methods to filtration. Unpublished Ph.D. thesis, Iowa State University, Ames, Iowa, 1978.

43. Saatci, A. M., and Oulman, C. S. The BDST method for deep bed filtration. Presented at the Second World Filtration Congress, London, 1979.

44. Saatci, A. M., and Oulman, C. S. The bed depth service time design method for deep bed filtration. J. AWWA, 72, (1980), 524-527.

45. Sakthivadivel, R., Thanikachalam, V., and Seetharaman, S. Head-loss theories in filtration. J. AWWA, 64 (4), (1972), 233-238.

46. Saleh, F. M. A. Theory of granular bed filtration and contact flocculation. Unpublished Ph.D. thesis, Iowa State University, Ames, Iowa, 1981.

47. Spielman, L. A. Particle capture mechanisms. In Deposition and Filtration of Particles from Gases and Liquids. London: Society of Chemical Industry, 1978.

48. Spielman, L. A., and Fitzpatrick, J. A. Theory for particle collection under London and gravity forces. J. Colloid Interface Sci., 42 (3), (1973), 607-623.

49. Stanley, D. R. Sand filtration studied with

radiotracers. Proc. ASCE, 81, (1955), 592-1-23.

50. Stein, P. C. A study of the theory of rapid filtration of water through sand. Doctoral dissertation, Massachusetts Institute of Technology, Cambridge, Mass., 1940.

51. Stumm, W., and Lee, G. F. Oxygenation of ferrous iron. Industrial and Engineering Chemistry, 53 (2), (1961), 143-146.

52. Stumm, W., and Morgan, J. J. Aquatic Chemistry. New York: Wiley-Interscience, 1981.

53. Tchobanoglous, G., and Eliassen, R. Filtration of treated sewage effluent. J. San. Eng. Div., Proc. ASCE, 96 (SA2), (1970), 243-265.

54. Thomas, H. C. Chromatography: A problem in kinetics. Ann. N.Y. Acad. Sci., 49, (1948), 161-182.

55. Tien, C., and Payatakes, A.C. Advances in deep bed filtration. J. AIChE, 25 (5), (1979), 737-759.

56. Tien, C., Turian, R. M., and Pendse, H. Simulation of the dynamic behavior of deep bed filters. J. AIChE, 25 (3), (1979), 385-395.

57. Water filtration-The Mints-Ives controversy 1960-73. J. Filtration & Separation, 13 (3), (1976), 131-133.

58. Yao, K-M., Habibian, M. T., and O'Melia, C. R. Water and waste water filtration: Concepts and applications. Environ. Sci. Technol., 5 (11), (1971), 1105-1112.

ACKNOWLEDGMENTS

The author wishes to thank Dr. C. S. Oulman for his guidance and helpful suggestions throughout this study. He also wishes to thank Dr. E. R. Baumann, Dr. J. L. Cleasby, Dr. H. T. David and Dr. B. R. Munson for serving on his committee. Special thanks are given to Roger Stephenson for his assistance in assembling the pilot filter system.

The author wishes to acknowledge the financial assistance he received from the Iowa State Engineering Research Institute as a graduate research assistant throughout most of the period of his graduate study.

Very special thanks go to his wife Tae-Hee for her understanding and encouragement, without which it would have been impossible to have carried on his graduate studies at Iowa State University. The author recognizes the difficulty that his sons, Jae and Seung-Min, had in adapting themselves to new environments, and he thanks them for their patience and understanding.

APPENDIX

Effects of Filtration Variables on the Filtration Coefficients

Regression analysis was used to determine the effects of influent iron concentration, C_o in mg/l, media size, D in mm, and filtration rate V in m/hr on the attachment coefficient K in l/g-hr and σ_u in g/l. The following equations demonstrate the results that were obtained for an 18-in depth of filter.

I. Effect of filtration rate (D = 0.841 mm)

A. C_o = 3.95 mg/l

$K = 138V^{-0.384}$ (R^2 = 99.5 %)

$\sigma_u = 0.396V^{0.602}$ (R^2 = 98.3 %)

B. C_o = 3.67 mg/l

$K = 468V^{-0.944}$ (R^2 = 90.9 %)

$\sigma_u = 0.386V^{0.68}$ (R^2 = 95.7 %)

C. C_o = 5.68 mg/l

$K = 74.1V^{-0.325}$ (R^2 = 72.2 %)

$\sigma_u = 0.228V^{0.893}$ (R^2 = 96.8 %)

D. C_o = 5.71 mg/l

$K = 19.05V^{-0.118}$ (R^2 = 19.3 %)

$\sigma_u = 0.681V^{0.44}$ (A^2 = 81.1 %)

E. C_o = 7.63 mg/l

$K = 102.3V^{-0.49}$ (R^2 = 97.5 %)

$\sigma_u = 0.309V^{0.942}$ (R^2 = 99.9 %)

F. C_o = 7.42 mg/l

$K = 45.7V^{-0.151}$ (R^2 = 24.5 %)

$\sigma_u = 0.647V^{0.674}$ (R^2 = 96.9 %)

II. Effect of media size (V = 14.67 m/hr)

A. C_o = 3.95 mg/l

$K = 41.7D^{0.453}$ (R^2 = 39.9 %)

$\sigma_u = 1.91D^{-0.819}$ (R^2 = 96.1 %)

B. C_o = 3.67 mg/l

$K = 25.7D^{-0.45}$ (R^2 = 52.4 %)

$\sigma_u = 2.5D^{-0.24}$ (R^2 = 93.2 %)

C. C_o = 5.68 mg/l

$K = 21.4D^{-0.813}$ (R^2 = 52.3 %)

$\sigma_u = 3.37D^{0.667}$ (R^2 = 54.5 %)

D. C_o = 5.71 mg/l

$K = 25.1D^{0.329}$ (R^2 =31.6 %)

$\sigma_u = 2.25D^{-0.25}$ (R^2 =32.7 %)

E. C_o = 7.63 mg/l

$K = 28.8D^{-0.0439}$ (R^2 = 24.2 %)

$\sigma_u = 3.6D^{-0.2}$ (R^2 = 89.6 %)

F. C_o = 7.42 mg/l

$K = 31.6D^{-0.764}$ (R^2 = 95.5 %)

$\sigma_u = 3.65D^{-0.285}$ (R^2 = 65.9 %)

III. Effect of influent concentration

A. D = 0.595 mm

V = 14.67 m/hr (6 gpm/ft^2)

$K = 18.2C_o^{0.283}$ (R^2 =8.4 %)

$\sigma_u = 2.11C_o^{0,213}$ (R^2 = 22.6 %)

B. D = 0.841 mm

V = 9.78 m/hr (4 gpm/ft^2)

$K = 177.8C_o^{-0.914}$ (R^2 = 62.5 %)

$\sigma_u = 0.583C_o^{0.744}$ (R^2 = 74.1 %)

C. D = 0.841 mm

V = 14.67 m/hr (6 gpm/ft^2)

$K = 63.1C_o^{-0.367}$ (R^2 = 33.7 %)

$\sigma_u = 0.866C_o^{0.663}$ (R^2 = 51 %)

D. D = 0.841 mm

V = 19.56 m/hr (8 gpm/ft^2)

$K = 72.4C_o^{-0.535}$ (R^2 = 54.3 %)

$\sigma_u = 0.701C_o^{0.925}$ (R^2 = 73.9 %)

E. D = 1.19 mm

V = 14.67 m/hr (6 gpm/ft^2)

$K = 28.2C_o^{-0.0602}$ (R^2 = 0.3 %)

$\sigma_u = 0.735C_o^{0.795}$ (R^2 = 50.6 %)

Derivation of Equations

Solutions of Filtration Equations (38)

The kinetic equation is:

$$\frac{\partial \sigma}{\partial t} = K(\sigma_u - \sigma)C \tag{45}$$

where

$$\sigma = \sigma(x,t)$$

$$C = C(x,t)$$

and the mass balance equation is:

$$\frac{\partial \sigma}{\partial t} + V \frac{\partial C}{\partial x} = 0 \tag{2}$$

with the following initial and boundary conditions:

$$C = C_o \quad \text{at} \quad x = 0, \quad t \geq 0$$

$$\sigma = \sigma_o \quad \text{at} \quad x = 0, \quad t \geq 0$$

$$\sigma = 0 \quad \text{at} \quad t = 0, \quad x \geq 0$$

Equation 45 is integrated at $x = 0$:

$$\int_0^{\sigma_o} \frac{d\sigma}{\sigma_u - \sigma} = \int_0^t KC_o \, dt$$

The result is:

$$-\ln\left[1 - \frac{\sigma_o}{\sigma_u}\right] = KC_o t$$

or

$$\frac{\sigma_o}{\sigma_u} = 1 - \exp\ (-KC_o t)$$

Combining Equations 45 and 2 at a given t:

$$-\frac{V}{C}\frac{dC}{dx} = K(\sigma_u - \sigma)$$

A mass balance over a filter depth, ℓ, for the time interval $[0,t]$ gives:

$$\int_0^t VC_o\ d\tau = \int_0^t VC(\ell,\tau)\ d\tau + \int_0^\ell \sigma(x,t)\ dx \qquad (76)$$

At the depth ℓ, the kinetic equation can be written in the following form:

$$C(\ell,\tau) = \frac{1}{K[\sigma_u - \sigma(\ell,\tau)]}\frac{\partial\sigma(\ell,\tau)}{\partial\tau}$$

Therefore,

$$\int_0^t VC(\ell,\tau)\ d\tau = \int_0^t \frac{V}{K[\sigma_u - \sigma(\ell,\tau)]}\frac{\partial\sigma(\ell,\tau)}{\partial\tau}\ d\tau$$

Then Equation 76 becomes:

$$\int_0^t VC_o \, d\tau = \int_0^{\sigma(\ell,t)} \frac{V \, d\sigma(\ell,\tau)}{K[\sigma_u - \sigma(\ell,\tau)]} + \int_0^{\ell} \sigma(x,t) \, dx$$

Differentiating with respect to ℓ and replacing ℓ by x:

$$0 = \frac{V}{K} \frac{1}{\sigma_u - \sigma(x,t)} \frac{d\sigma(x,t)}{dx} + \sigma(x,t)$$

or

$$- \frac{V}{\sigma(x,t)} \frac{d\sigma(x,t)}{dx} = K[\sigma_u - \sigma(x,t)]$$

Thus,

$$- \frac{V}{\sigma} \frac{d\sigma}{dx} = - \frac{V}{C} \frac{dC}{dx}$$

or

$$\int_{\sigma_o}^{\sigma} \frac{d\sigma}{\sigma} = \int_{C_o}^{C} \frac{dC}{C}$$

or

$$\ln (\sigma/\sigma_o) = \ln (C/C_o)$$

or

$$\sigma/\sigma_o = C/C_o$$

Again returning to:

$$-\frac{V}{\sigma}\frac{d\sigma}{dx} = K(\sigma_u - \sigma)$$

and integrating:

$$\int_{\sigma_o}^{\sigma} \frac{d\sigma}{\sigma(\sigma_u - \sigma)} = -\int_0^x \frac{K}{V}\, dx$$

yields:

$$I_I = -Kx/V$$

where

$$I_I = \int_{\sigma_o}^{\sigma} \frac{d\sigma}{\sigma(\sigma_u - \sigma)}$$

If

$$w = \sigma/\sigma_u$$
$$\sigma = \sigma_u w$$
$$d\sigma = \sigma_u\, dw$$

then,

$$I_I = \frac{1}{\sigma_u}\int_{w_o}^{w} \frac{dw}{w(1 - w)}$$

$$= \frac{1}{\sigma_u}[\ln w - \ln (1 - w)]\Big|_{\sigma_o/\sigma_u}^{\sigma/\sigma_u}$$

$$= \frac{1}{\sigma_u} \ln \left[\frac{\sigma/\sigma_u}{\sigma_o/\sigma_u} \frac{1 - \sigma_o/\sigma_u}{1 - \sigma/\sigma_u}\right]$$

Thus,

$$\frac{\frac{\sigma/\sigma_u}{\sigma_o/\sigma_u}}{1 - \sigma/\sigma_u} = [\exp (-\sigma_u Kx/V)](1 - \sigma_o/\sigma_u)^{-1}$$

$$= \exp (-\sigma_u Kx/V) \exp (KC_o t)$$

$$= \exp (-\sigma_u Kx/V + KC_o t)$$

Multiplying through by σ_o/σ_u:

$$\frac{\sigma/\sigma_u}{1 - \sigma/\sigma_u} = (\sigma_o/\sigma_u) \exp (-\sigma_u Kx/V + KC_o t)$$

Rearranging:

$$\sigma/\sigma_u = \frac{(\sigma_o/\sigma_u) \exp (-\sigma_u Kx/V + KC_o t)}{1 + (\sigma_o/\sigma_u) \exp (-\sigma_u Kx/V + KC_o t)}$$

Since $\sigma_o/\sigma_u = 1 - \exp(-KC_o t)$,

$$\sigma/\sigma_u = \frac{[1 - \exp(-KC_o t)][\exp(-\sigma_u Kx/V + KC_o t)]}{1 + [1 - \exp(-KC_o t)][\exp(-\sigma_u Kx/V + KC_o t)]}$$

Therefore,

$$\sigma = \frac{\sigma_u[1 - \exp(-KC_o t)]}{\exp(Kx\sigma_u/V - KC_o t) - \exp(-KC_o t) + 1} \qquad (47)$$

Since $\sigma_o = \sigma_u[1 - \exp(-KC_o t)]$,

$$\sigma = \frac{\sigma_o}{\exp(Kx\sigma_u/V - KC_o t) - \exp(-KC_o t) + 1}$$

Since $\sigma/\sigma_o = C/C_o$,

$$C = \frac{C_o}{\exp(Kx\sigma_u/V - KC_o t) - \exp(-KC_o t) + 1} \qquad (46)$$

Equations 46 and 47 are essentially identical to those in Heertjes and Lerk's model (Equations 19 and 20) which were derived starting with a different kinetic equation.

Rearranging Equation 46:

$$\frac{C_o}{C} = \exp(Kx\sigma_u/V - KC_o t) - \exp(-KC_o t) + 1$$

or

$$\frac{C_o}{C} - 1 = \frac{\exp\ (Kx\sigma_u/V) - 1}{\exp\ (KC_o t)}$$

or

$$-\ln\left[\frac{C_o}{C} - 1\right] = -\ln\ [\exp\ (Kx\sigma_u/V) - 1] + KC_o t \qquad (48)$$

Derivation of head loss equation

$$H = H_o + a\int_0^L \sigma\ dx$$

Using Equation 47 for σ, the integral becomes:

$$\int_0^L \sigma\ dx = \int_0^L \frac{\sigma_u[1 - \exp\ (-KC_o t)]\ dx}{\exp\ (Kx\sigma_u/V - KC_o t) - \exp\ (-KC_o t) + 1}$$

$$= \sigma_u[\exp\ (KC_o t) - 1]\int_0^L \frac{dx}{\exp\ (Kx\sigma_u/V) - 1 + \exp\ (KC_o t)}$$

If

$$q = 1$$

$$b = K\sigma_u/V$$

$$p = -1 + \exp\ (KC_o t)$$

then,

$$I_{II} = \int_0^L \frac{dx}{\exp\ (Kx\sigma_u/V) - 1 + \exp\ (KC_o t)}$$

$$= \int_0^L \frac{dx}{p + q\ \exp\ (bx)}$$

Since

$$\int \frac{dx}{p + q\ \exp\ (bx)} = \frac{1}{bp}\left[bx - \ln\ [p + q\ \exp\ (bx)]\right],$$

$$I_{II} = \frac{1}{(K\sigma_u/V)\,[\exp\ (KC_o t) - 1]}\left[K\sigma_u x/V - \ln [\exp\ (KC_o t) - 1 + \exp\ (K\sigma_u x/V)]\right]\Bigg|_0^L$$

or

$$I_{II} = \frac{1}{(K\sigma_u/V)\,[\exp\ (KC_o t) - 1]}\left[K\sigma_u L/V - \ln [\exp\ (KC_o t) - 1 + \exp\ (K\sigma_u L/V)] + KC_o t\right]$$

Therefore,

$$H = H_o + a\left[\sigma_u L - \frac{V}{K} \ln\ [\exp(KC_o t) + \exp\ (K\sigma_u L/V) - 1] + C_o V t\right] \qquad (52)$$

Worked Example of Data Analysis

A worked example of data analysis will be shown using the data from Filter A of Run 10. Effluent data are listed in Table 13 along with values for $-\ln (C_o - C)$ used in linearizing the data. A plot of the linearized data is shown in Figure 24. Data at $t = 0$, 0.75 and 1.5 hr will be ignored since they belong to the ripening period. The regression line for the data that was used is:

$$-\ln (C_o/C - 1) = -3.06 + 0.222t$$

The intercept, A, and the slope, B, are therefore:

$$A = -3.06$$

$$B = 0.222 \text{ hr}^{-1}$$

Therefore,

$$K = \frac{B}{C_o}$$

$$= \frac{0.222 \text{ hr}^{-1}}{7.63 \times 10^{-3} \text{ g/l}}$$

$$= 29.1 \text{ l/g-hr}$$

and

$$\sigma_u = \frac{V}{Kx} \ln (e^{-A} + 1)$$

$$= \frac{14.67 \text{ m/hr}}{(29.1 \text{ l/g-hr})(0.4572 \text{ m})} \ln (e^{3.06} + 1)$$

$$= 1.627 \text{ g/l}$$

Table 13. Effluent data for Filter A of Run 10[a]

t hours	C mg/l as Fe	$-\ln (C_o/C - 1)$
0	2.8	-0.545
0.75	0.95	-1.95
1.5	0.62	-2.42
2.25	0.59	-2.48
3	0.64	-2.39
3.75	0.69	-2.31
4.5	0.81	-2.13
5.25	1.01	-1.88
6	1.18	-1.698
6.75	1.32	-1.565
7.5	1.56	-1.361
8.25	1.72	-1.237

[a]Mean C_o = 7.63 mg/l as Fe.

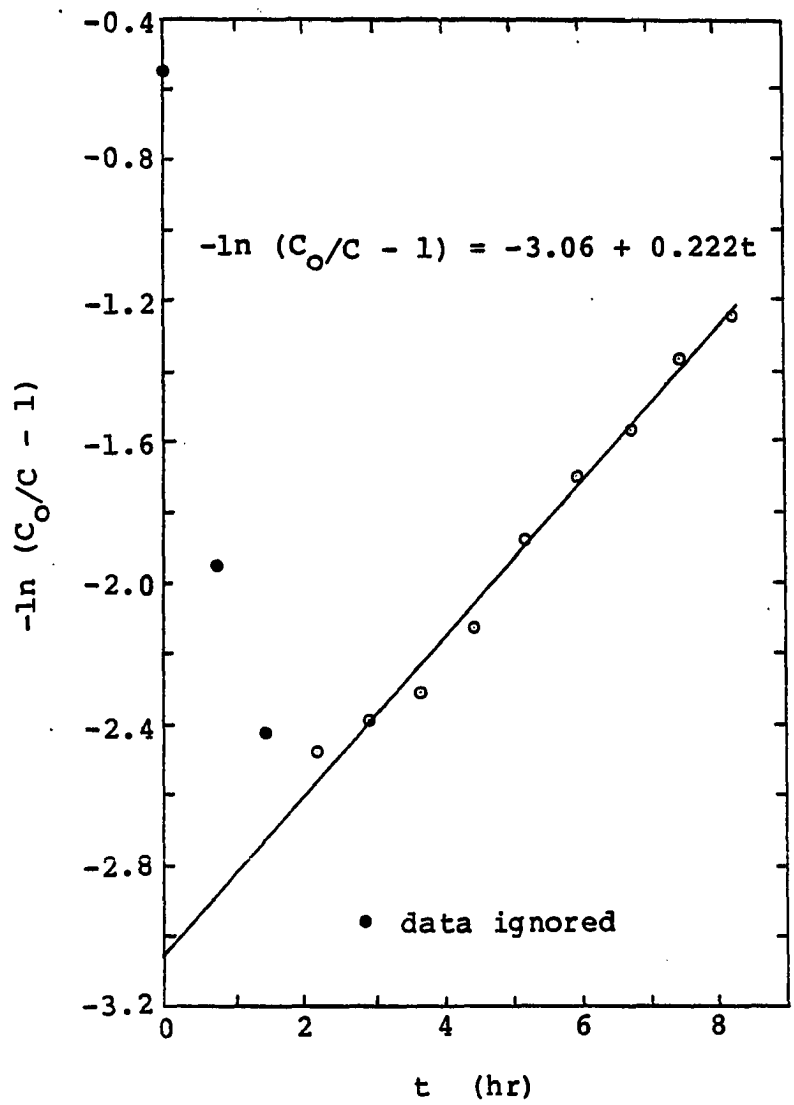

Figure 24. Linearization of data from Filter A of Run 10

Data from 18-in Depth Filter Runs

Table 14a. Iron concentration for Run 9 (L = 18 in, mean C_o = 3.95 mg/l as Fe)

Time	Influent conc.	Effluent conc., mg/l				
hr	mg/l	A	B	C	D	E
0	3.75	2.08	1.22	1.72	2.16	1.28
0.75	3.84	2.73	1.03	1.5	1.92	1.05
1.5	3.8	1.63	0.71	1.04	1.36	0.63
2.25	3.8	1.4	0.68	0.92	—	0.49
3	3.8	1.55	0.44	0.75	1.12	0.48
3.75	3.86	1.64	0.33	0.67	0.91	0.46
4.5	3.88	1.12	0.32	0.62	0.92	0.47
5.25	4	1.12	0.37	0.52	0.92	0.44
6	3.88	1.12	0.24	0.55	1.1	0.48
6.75	3.94	1.1	0.29	0.58	1	0.52
7.5	4	1.21	0.3	0.67	1.08	0.53
8.25	4	1.37	0.38	0.68	1.12	0.55
9	4.04	1.32	0.4	0.91	1.22	0.63
9.75	3.98	1.45	0.56	0.81	1.37	0.68
10.5	4.06	1.71	0.58	1.03	1.45	0.69
11.25	4	—	0.8	—	1.76	0.83
12	4.12	1.77	0.69	1.3	1.74	0.82
12.75	4	1.99	0.75	1.36	1.87	0.9
13.5	4	2.33	0.99	1.65	2.1	1.0
14.25	4.06	—	1.22	1.8	2.26	1.05
15	4.14	2.52	—	—	2.33	1.06

Table 14b. Increment of head loss for Run 9 (L = 18 in, mean C_o = 3.95 mg/l as Fe)

Time	Head loss increment, mm				
hr	A	B	C	D	E
0	0	0	0	0	0
0.75	7	11	12	15	22
1.5	14	17	31	36	47
2.25	23	28	51	63	78
3	40	37	78	95	123
3.75	48	54	109	133	167
4.5	65	—	126	170	216
5.25	79	86	158	218	270
6	91	109	189	264	326
6.75	118	132	234	317	401
7.5	131	154	268	358	458
8.25	151	181	322	407	528
9	169	207	349	476	596
9.75	197	235	420	539	691
10.5	217	259	457	558	784
11.25	228	288	495	652	856
12	250	316	538	725	990
12.75	270	343	597	795	1091
13.5	300	356	678	879	1216
14.25	304	392	695	954	1344
15	324	434	790	1015	1445

Table 15a. Iron concentration for Run 16 (L = 18 in, mean C_o = 3.67 mg/l as Fe)

Time	Influent conc.	Effluent conc., mg/l				
hr	mg/l	A	B	C	D	E
0	3.5	1.79	0.81	1.46	1.95	1.22
0.75	3.6	1.98	1.08	1.5	1.92	1.12
1.5	3.6	1.72	0.78	1.14	1.53	0.78
2.25	3.5	1.49	0.55	0.89	1.28	0.6
3	3.6	1.36	0.42	0.71	1.07	0.5
3.75	3.6	1.21	0.35	0.63	1.05	0.47
4.5	3.6	1.32	0.37	0.75	—	0.56
5.25	3.66	1.17	0.35	0.67	0.99	0.5
6	3.6	1.17	0.32	0.63	1.04	0.58
6.75	3.6	1.22	0.29	0.63	1.0	0.57
7.5	3.7	1.15	0.29	0.63	1.08	0.58
8.25	3.68	1.24	0.28	0.63	1.11	0.58
9	3.66	1.18	0.28	0.73	1.12	0.63
9.75	3.65	1.27	0.32	0.8	1.17	0.66
10.5	3.7	1.27	0.48	0.73	1.19	0.66
11.25	3.76	1.43	0.28	0.8	—	0.68
12	3.76	1.38	0.33	1.08	1.35	0.81
12.75	3.6	1.49	0.52	0.88	1.42	0.85
13.5	3.7	1.42	0.51	1.12	1.47	0.9
14.25	3.92	1.52	0.48	1.09	1.62	0.98
15	3.76	1.62	0.53	1.3	1.7	1.07
15.75	3.74	1.72	0.78	1.28	1.74	1.07
16.5	3.76	1.62	0.73	1.31	1.81	1.12
17.25	3.76	—	0.93	1.45	—	1.14

Table 15b. Increment of head loss for Run 16 (L = 18 in, mean C_o = 3.67 mg/l as Fe)

Time	Head loss increment, mm				
hr	A	B	C	D	E
0	0	0	0	0	0
0.75	4	5	12	22	17
1.5	8	14	20	37	45
2.25	20	15	36	54	73
3	24	31	50	77	101
3.75	35	35	64	98	134
4.5	40	45	82	128	168
5.25	51	52	102	155	215
6	60	64	124	184	243
6.75	71	72	146	214	285
7.5	89	90	166	257	341
8.25	100	113	197	294	387
9	113	117	227	319	439
9.75	120	156	255	359	494
10.5	141	177	280	403	539
11.25	149	181	—	432	594
12	164	203	333	474	641
12.75	176	223	376	505	692
13.5	192	236	388	550	749
14.25	211	251	420	584	796
15	220	288	439	622	838
15.75	230	296	463	649	902
16.5	240	312	491	697	961
17.25	—	321	505	—	993
18	—	347	543	—	1076

Table 16a. Iron concentration for Run 12 (L = 18 in, mean C_o = 5.68 mg/l as Fe)

Time	Influent conc.	Effluent conc., mg/l				
hr	mg/l	A	B	C	D	E
0	5.5	2.28	1.17	1.56	1.85	0.72
0.75	5.55	1.03	0.57	0.65	0.81	0.46
1.5	5.6	0.72	0.43	0.61	0.77	0.63
2.25	5.65	0.7	0.48	0.71	0.9	0.82
3	5.75	0.87	0.53	0.82	1.05	0.98
3.75	5.65	0.89	0.61	—	1.18	1.06
4.5	—	0.98	0.71	1.02	1.23	1.12
5.25	5.8	1.0	0.7	1.13	1.31	1.16
6	5.8	1.08	0.93	1.46	1.42	1.2
6.75	5.5	1.15	0.95	1.53	1.52	1.33
7.5	5.6	1.21	0.99	1.37	1.47	1.24
8.25	5.8	1.26	1.0	1.26	1.52	1.2
9	5.85	1.33	1.1	1.4	1.5	1.22
9.75	5.8	1.58	1.15	1.58	1.59	1.26
10.5	—	1.68	1.28	1.53	1.68	1.32

Table 16b. Increment of head loss for Run 12 (L = 18 in, mean C_o = 5.68 mg/l as Fe)

Time	Head loss increment, mm				
hr	A	B	C	D	E
0	0	0	0	0	0
0.75	16	23	47	52	62
1.5	46	53	93	123	143
2.25	72	85	146	205	—
3	106	117	213	290	352
3.75	137	161	269	377	473
4.5	161	181	332	470	607
5.25	195	236	420	578	748
6	211	277	490	693	908
6.75	248	314	553	795	1055
7.5	284	355	610	899	1225
8.25	320	401	722	1036	1401
9	356	442	779	1165	1583
9.75	392	491	876	1277	1748
10.5	432	538	970	1418	1940

Table 17a. Iron concentration for Run 15 (L = 18 in, mean C_o = 5.71 mg/l as Fe)

Time	Influent conc.	Effluent conc., mg/l				
hr	mg/l	A	B	C	D	E
0	5.35	2.57	1.32	1.86	2.49	1.11
0.75	5.45	1.8	1.12	1.28	1.52	0.92
1.5	5.5	1.4	0.8	1.12	1.37	1.12
2.25	5.6	1.32	0.9	1.27	1.45	1.26
3	5.7	1.41	0.98	1.37	1.7	1.47
3.75	5.85	1.47	1.01	1.52	1.86	1.62
4.5	5.75	1.59	1.1	1.6	1.91	1.76
5.25	—	1.75	1.26	1.83	2.12	1.82
6	5.75	1.91	1.34	1.96	2.22	1.96
6.75	6.1	—	1.43	2.08	—	—
7.5	6	2.14	1.46	2.00	2.44	1.98
8.25	5.75	—	1.56	—	2.62	2.04
9	—	—	1.8	—	2.9	2.1

Table 17b. Increment of head loss for Run 15 (L = 18 in, mean C_o = 5.71 mg/l as Fe)

Time	Head loss increment, mm				
hr	A	B	C	D	E
0	0	0	0	0	0
0.75	12	15	31	40	46
1.5	29	31	65	90	102
2.25	52	54	107	150	176
3	81	85	161	224	246
3.75	103	104	206	288	330
4.5	128	133	256	358	433
5.25	144	155	302	422	522
6	—	—	—	501	633
6.75	188	211	414	571	730
7.5	217	240	479	646	840
8.25	—	263	—	714	946
9	—	284	—	786	1048

Table 18a. Iron concentration for Run 10 (L = 18 in, mean C_o = 7.63 mg/l as Fe)

Time	Influent conc.	Effluent conc., mg/l				
hr	mg/l	A	B	C	D	E
0	7.63	2.8	1.22	1.66	2.14	0.76
0.75	7.55	0.95	0.33	0.46	0.72	0.27
1.5	—	0.62	0.19	0.38	0.59	0.23
2.25	7.45	0.59	0.22	0.37	0.67	0.32
3	7.5	0.64	0.27	0.48	0.74	0.41
3.75	7.75	0.69	0.27	0.52	0.88	0.48
4.5	7.55	0.81	0.42	0.72	1.02	0.53
5.25	8	1.01	0.47	0.89	1.17	0.62
6	7.85	1.18	0.59	0.95	1.26	0.62
6.75	7.5	1.32	0.66	1.02	1.33	—
7.5	7.55	1.56	0.72	1.1	1.42	—
8.25	7.7	1.72	0.85	1.42	1.65	—
9	7.55	—	1.12	1.3	1.92	—

Table 18b. Increment of head loss for Run 10 (L = 18 in, mean C_o = 7.63 mg/l as Fe)

Time	Head loss increment, mm				
hr	A	B	C	D	E
0	0	0	0	0	0
0.75	33	37	58	77	101
1.5	77	98	143	183	218
2.25	124	155	251	301	394
3	157	201	353	452	598
3.75	215	276	459	600	807
4.5	275	336	610	775	1056
5.25	332	421	765	970	1346
6	391	483	903	1167	1643
6.75	455	567	1075	1388	—
7.5	528	671	1245	1635	—
8.25	598	745	1416	1876	—
9	—	870	1585	2118	—

Table 19a. Iron concentration for Run 14 (L = 18 in, mean C_o = 7.42 mg/l as Fe)

Time	Influent conc.	Effluent conc., mg/l				
hr	mg/l	A	B	C	D	E
0	7.15	1.9	0.9	1.12	1.42	0.44
0.75	7.15	0.72	0.23	0.32	0.55	0.15
1.5	7.15	0.5	0.12	0.23	0.42	0.12
2.25	7.25	0.44	0.11	0.22	0.43	0.15
3	7.5	0.5	0.11	0.26	0.53	0.23
3.75	7.25	0.56	0.2	0.33	0.65	0.32
4.5	7.6	0.62	0.22	0.42	0.81	0.42
5.25	7.8	0.76	0.3	0.55	0.83	0.4
6	7.4	0.88	0.34	0.76	1.1	0.63
6.75	7.5	1.28	0.4	0.7	1.03	—
7.5	7.85	1.3	0.43	—	1.35	0.95
8.25	7.4	1.19	0.55	0.93	—	—
9	—	1.46	0.62	0.99	—	—

Table 19b. Increment of head loss for Run 14 (L = 18 in, mean C_o = 7.42 mg/l as Fe)

Time	Head loss increment, mm				
hr	A	B	C	D	E
0	0	0	0	0	0
0.75	31	35	59	84	113
1.5	71	75	128	184	225
2.25	123	127	222	321	394
3	165	175	324	440	598
3.75	213	248	453	603	855
4.5	265	329	574	758	1125
5.25	336	404	710	983	1411
6	391	480	884	1211	1853
6.75	451	556	1032	1443	2183
7.5	517	641	1182	1693	2533
8.25	591	734	1379	—	2888
9	660	802	1536	—	3307